

# Bayesian Optimization-based Combinatorial Assignment

Jakob Weissteiner<sup>1,3\*</sup> Jakob Heiss<sup>2,3\*</sup> Julien Siems<sup>1\*</sup> Sven Seuken<sup>1,3</sup>

<sup>1</sup>UNIVERSITY OF ZURICH

<sup>2</sup>ETH ZURICH

<sup>3</sup>ETH AI CENTER

*weissteiner@ifi.uzh.ch, jakob.heiss@math.ethz.ch, juliensiem@gmail.com, seuken@ifi.uzh.ch*

## Abstract

We study the combinatorial assignment domain, which includes combinatorial auctions and course allocation. The main challenge in this domain is that the bundle space grows exponentially in the number of items. To address this, several papers have recently proposed *machine learning-based preference elicitation* algorithms that aim to elicit only the most important information from agents. However, the main shortcoming of this prior work is that it does not model a mechanism’s uncertainty over values for not yet elicited bundles. In this paper, we address this shortcoming by presenting a *Bayesian Optimization-based Combinatorial Assignment (BOCA)* mechanism. Our key technical contribution is to integrate a method for capturing model uncertainty into an iterative combinatorial auction mechanism. Concretely, we design a new method for estimating an *upper uncertainty bound* that can be used as an acquisition function to determine the next query to the agents. This enables the mechanism to properly *explore* (and not just *exploit*) the bundle space during its preference elicitation phase. We run computational experiments in several spectrum auction domains to evaluate BOCA’s performance. Our results show that BOCA achieves higher allocative efficiency than state-of-the-art approaches.

## 1 Introduction

Many economic problems require finding an efficient combinatorial assignment of multiple indivisible items to multiple agents. Popular examples include *combinatorial auctions (CAs)*, *combinatorial exchanges (CEs)*, and *combinatorial course allocation*. In CAs, heterogeneous items are allocated among a set of bidders, e.g., for the sale of spectrum licenses (Cramton 2013). In CEs, items are allocated among agents who can be sellers *and* buyers at the same time, e.g., for the re-allocation of catch shares (Bichler, Fux, and Goeree 2019). In course allocation, course seats are allocated among students at universities (Budish 2011).

In all these domains, agents have preferences over *bundles* of items. In particular, agents’ preferences may exhibit *complementarities* and *substitutabilities* among items. A mechanism that allows agents to report values for bundles rather than just for individual items can achieve significantly higher efficiency. However, this also implies that agents’ preferences are exponentially-sized (i.e., for  $m$  items there

are  $2^m$  different bundles), which implies that agents cannot report values for all bundles. Therefore, the key challenge in combinatorial assignment is the design of a *preference elicitation (PE)* algorithm that is (i) *practically feasible* w.r.t. elicitation costs and (ii) *smart*, i.e., it should elicit the information that is “most useful” for achieving high efficiency.

### 1.1 Iterative Combinatorial Auctions (ICAs)

While the PE challenge is common to all combinatorial assignment problems, it has been studied most intensely in the CA domain (Sandholm and Boutilier 2006). In CAs with general valuations, the amount of communication needed to guarantee full efficiency is exponential in the number of items (Nisan and Segal 2006). Thus, practical CAs cannot provide efficiency guarantees. In practice, *iterative combinatorial auctions (ICAs)* are therefore employed, where the auctioneer interacts with bidders over rounds, eliciting a *limited* (and thus *practically feasible*) amount of information, aiming to find a highly efficient allocation. ICAs are widely used; e.g., for the sale of licenses to build offshore wind farms (Ausubel and Cramton 2011). The provision of spectrum licenses via the *combinatorial clock auction (CCA)* (Ausubel, Cramton, and Milgrom 2006) has generated more than \$20 billion in total revenue (Ausubel and Baranov 2017). Thus, increasing the efficiency of such real-world ICAs by only 1% point translates into monetary gains of hundreds of millions of dollars.

### 1.2 ML-powered Preference Elicitation

In recent years, researchers have used machine learning (ML) to design smart PE algorithms. Most related to this paper is the work by Brero, Lubin, and Seuken (2018, 2021), who developed the first practical ML-powered ICA that outperforms the CCA. The main idea of their mechanism is two-fold: first, they train a separate *support vector regression* model to learn each bidder’s full value function from a small set of bids; second, they solve an *ML-based winner determination problem (WDP)* to determine the allocation with the highest predicted social welfare, and they use this allocation to generate the next set of queries to all bidders. This process repeats in an iterative fashion until a fixed number of queries have been asked. Thus, their ML-powered ICA can be interpreted as a form of combinatorial *Bayesian Optimization (BO)* (see Appendix C for details).

\*These authors contributed equally.

In several follow-up papers, this work has been extended by developing more sophisticated ML methods for this problem. Weissteiner and Seuken (2020) integrated *neural networks (NN)* in their ICA and further increased efficiency. Weissteiner et al. (2022b) used *Fourier transforms (FTs)* to leverage different notions of sparsity of value functions. Finally, Weissteiner et al. (2022a) achieved state-of-the-art (SOTA) performance using *Monotone-Value NNs (MVNNs)*, which incorporate important prior domain knowledge.

The main shortcoming of this prior work is that all of these approaches are *myopic* in the sense that the resulting mechanisms simply query the allocation with the highest predicted welfare. In particular, the mechanisms do not have any model of *uncertainty* over bidders’ values for not yet elicited bundles, although handling uncertainty in a principled manner is one of the key requirements of a smart PE algorithm (Bonilla, Guo, and Sanner 2010). Thus, the mechanisms cannot properly control the *exploration-exploitation trade-off* inherent to BO. For ML-based ICAs, this means that the mechanisms may get stuck in local minima, repeatedly querying one part of the allocation space while not exploring other, potentially more efficient allocations.

### 1.3 Our Contributions

In this paper, we address this main shortcoming of prior work and show how to integrate a notion of *model uncertainty* (i.e., epistemic uncertainty) over agents’ preferences into iterative combinatorial assignment. Concretely, we design a *Bayesian Optimization-based combinatorial assignment (BOCA)* mechanism that makes use of model uncertainty in its query generation module. The main technical challenge is to design a new method for estimating an *upper uncertainty bound* that can be used as an acquisition function to determine the next query. To this end, we combine *MVNNs* (Weissteiner et al. 2022a) with *Neural optimization-based Model Uncertainty (NOMU)* (Heiss et al. 2022), a recently introduced method to estimate model uncertainty for NNs. In detail, we make the following contributions:

1. We present a modified NOMU algorithm (Section 3.1), tailored to CAs, exploiting monotonicity of agents’ preferences and the discrete (finite) nature of this setting.
2. We show that generic parameter initialization for monotone NNs can dramatically fail and propose a new initialization method for MVNNs based on uniform mixture distributions (Section 3.2).
3. We present a more succinct mixed integer linear program for MVNNs to solve the ML-based WDP (Section 3.3).
4. We experimentally show that BOCA outperforms prior approaches in terms of efficiency (Section 4).

Although our contribution applies to any combinatorial assignment setting, we focus on CAs to simplify the notation and because there exist well-studied preference generators for CAs that we use for our experiments.

### 1.4 Related Work on Model Uncertainty

Estimating model uncertainty for NNs is an active area of research in AI and ML, with a plethora of new methods

proposed every year. Classic methods can be broadly categorized into (i) *ensemble methods*: training multiple different NNs to estimate model uncertainty (Gal and Ghahramani 2016; Lakshminarayanan, Pritzel, and Blundell 2017; Wenzel et al. 2020) and (ii) *Bayesian NNs (BNNs)*: assuming a prior distribution over parameters and then estimating model uncertainty by approximating the intractable posterior (Graves 2011; Blundell et al. 2015; Hernández-Lobato and Adams 2015; Ober and Rasmussen 2019). However, for ML-based iterative combinatorial assignment, a key requirement is to be able to efficiently solve the ML-based WDP based on these uncertainty estimates. As there is no known computationally tractable method to perform combinatorial optimization over ensembles or BNNs, we cannot use these approaches for ML-based ICAs. In contrast, NOMU (Heiss et al. 2022) enables the computationally efficient optimization over its uncertainty predictions, which is why we use it as a building block for BOCA.

## 2 Preliminaries

In this section, we present our formal model (Section 2.1) and review the ML-based ICA by Brero, Lubin, and Seuken (2021) (Section 2.2), *monotone-value neural networks (MVNNs)* by Weissteiner et al. (2022a) (Section 2.3), and *neural optimization-based model uncertainty (NOMU)* by Heiss et al. (2022) (Section 2.4).

### 2.1 Formal Model for ICAs

We consider a CA with  $n$  bidders and  $m$  indivisible items. Let  $N = \{1, \dots, n\}$  and  $M = \{1, \dots, m\}$  denote the set of bidders and items. We denote by  $x \in \mathcal{X} = \{0, 1\}^m$  a bundle of items represented as an indicator vector, where  $x_j = 1$  iff item  $j \in M$  is contained in  $x$ . Bidders’ true preferences over bundles are represented by their (private) value functions  $v_i : \mathcal{X} \rightarrow \mathbb{R}_+$ ,  $i \in N$ , i.e.,  $v_i(x)$  represents bidder  $i$ ’s true value for bundle  $x \in \mathcal{X}$ .

By  $a = (a_1, \dots, a_n) \in \mathcal{X}^n$  we denote an allocation of bundles to bidders, where  $a_i$  is the bundle bidder  $i$  obtains. We denote the set of *feasible* allocations by  $\mathcal{F} = \{a \in \mathcal{X}^n : \sum_{i \in N} a_{ij} \leq 1, \forall j \in M\}$ . We assume that bidders have quasilinear utility functions  $u_i$ , i.e., for payments  $p \in \mathbb{R}_+^n$ ,  $u_i(a, p) = v_i(a_i) - p_i$ . This implies that the (true) *social welfare*  $V(a)$  of an allocation  $a$  is equal to the sum of all bidders’ values  $\sum_{i \in N} v_i(a_i)$ . We let  $a^* \in \operatorname{argmax}_{a \in \mathcal{F}} V(a)$  denote a social-welfare maximizing, i.e., *efficient*, allocation. The *efficiency* of any allocation  $a \in \mathcal{F}$  is determined as  $V(a)/V(a^*)$ .

An ICA *mechanism* defines how the bidders interact with the auctioneer and how the allocation and payments are determined. We denote a bidder’s (possibly untruthful) reported value function by  $\hat{v}_i : \mathcal{X} \rightarrow \mathbb{R}_+$ . In this paper, we consider ICAs that ask bidders to iteratively report their values  $\hat{v}_i(x)$  for bundles  $x$  selected by the mechanism. A finite set of reported bundle-value pairs of bidder  $i$  is denoted as  $R_i = \{(x^{(l)}, \hat{v}_i(x^{(l)}))\}$ ,  $x^{(l)} \in \mathcal{X}$ . Let  $R = (R_1, \dots, R_n)$  be the tuple of reported bundle-value pairs obtained from all bidders. We define the *reported social welfare* of an allocation  $a$  given  $R$  as  $\widehat{V}(a|R) := \sum_{i \in N: (a_i, \hat{v}_i(a_i)) \in R_i} \hat{v}_i(a_i)$ ,

where  $(a_i, \hat{v}_i(a_i)) \in R_i$  ensures that only values for reported bundles contribute. The ICA’s optimal allocation  $a_R^* \in \mathcal{F}$  and payments  $p(R) \in \mathbb{R}_+^n$  are computed based on the elicited reports  $R$  only. More formally,  $a_R^* \in \mathcal{F}$  given reports  $R$  is defined as

$$a_R^* \in \operatorname{argmax}_{a \in \mathcal{F}} \widehat{V}(a|R). \quad (1)$$

As the auctioneer can only query a limited number of bundles  $|R_i| \leq Q^{\max}$  (e.g.,  $Q^{\max} = 100$ ), an ICA needs a practically feasible and smart PE algorithm.

## 2.2 A Machine Learning-powered ICA

We now provide a high-level review of the *machine learning-powered combinatorial auction (MLCA)* by [Brero, Lubin, and Seuken \(2021\)](#) (please see Appendix A for further details). MLCA proceeds in rounds until a maximum number of value queries per bidder  $Q^{\max}$  is reached. In each round, for every bidder  $i$ , an ML model  $\mathcal{A}_i$  is trained on the bidder’s reports  $R_i$ . Next, MLCA generates new value queries by computing the allocation with the highest predicted social welfare. Concretely, it computes  $q^{\text{new}} = (q_i^{\text{new}})_{i=1}^n$  with  $q_i^{\text{new}} \in \mathcal{X} \setminus R_i$  by solving an ML-based WDP:

$$q^{\text{new}} \in \operatorname{argmax}_{a \in \mathcal{F}} \sum_{i \in N} \mathcal{A}_i(a_i) \quad (2)$$

The idea is the following: if the  $\mathcal{A}_i$ ’s are good surrogate models of the bidders’ value functions, then the efficiency of  $q^{\text{new}}$  is likely to be high as well. Thus, in each round, bidders are providing value reports on bundles that are guaranteed to fit into a feasible allocation and that together are predicted to have high social welfare. Additionally, bidders are also allowed to submit “push-bids,” enabling them to submit information to the auctioneer that they deem useful, even if they are not explicitly queried about it. At the end of each round, MLCA receives reports  $R^{\text{new}}$  from all bidders for the newly generated queries  $q^{\text{new}}$ , and updates the overall elicited reports  $R$ . When  $Q^{\max}$  is reached, MLCA computes an allocation  $a_R^*$  that maximizes the *reported* social welfare (Equation (1)) and determines VCG payments  $p(R)$  based on all reports (see Appendix Definition B.1).

**Remark 1** (IR, No-Deficit, and Incentives of MLCA). [Brero, Lubin, and Seuken \(2021\)](#) showed that MLCA satisfies individual rationality (IR) and no-deficit, with any ML algorithm. They also studied MLCA’s incentive properties; this is important, since manipulations may lower efficiency. Like all deployed ICAs (including the CCA), MLCA is not strategyproof. However, they argued that it has good incentives in practice; and given two additional assumptions, bidding truthfully is an ex-post Nash equilibrium. We present a detailed summary of their incentive analysis in Appendix B.

## 2.3 MVNNs: Monotone-Value Neural Networks

MVNNs ([Weissteiner et al. 2022a](#)) are a new class of NNs that is specifically designed to represent *monotone combinatorial* valuations. First, we reprint the definition of MVNNs and then discuss their desirable properties.

**Definition 1** (MVNN, [Weissteiner et al. \(2022a\)](#)). An MVNN  $\mathcal{M}_i^\theta : \mathcal{X} \rightarrow \mathbb{R}_+$  for bidder  $i \in N$  is defined as

$$\mathcal{M}_i^\theta(x) := W^{i,K_i} \varphi_{0,t^i,K_i-1}(\dots \varphi_{0,t^i,1}(W^{i,1}x + b^{i,1}) \dots) \quad (3)$$

- $K_i + 1 \in \mathbb{N}$  is the number of layers ( $K_i - 1$  hidden layers),
- $\{\varphi_{0,t^i,k}\}_{k=1}^{K_i-1}$  are the MVNN-specific activation functions with cutoff  $t^{i,k} > 0$ , called bounded ReLU (bReLU):

$$\varphi_{0,t^i,k}(\cdot) := \min(t^{i,k}, \max(0, \cdot)) \quad (4)$$

- $W^i := (W^{i,k})_{k=1}^{K_i}$  with  $W^{i,k} \geq 0$  and  $b^i := (b^{i,k})_{k=1}^{K_i-1}$  with  $b^{i,k} \leq 0$  are the non-negative weights and non-positive biases of dimensions  $d^{i,k} \times d^{i,k-1}$  and  $d^{i,k}$ , whose parameters are stored in  $\theta = (W^i, b^i)$ .

MVNNs are particularly well suited for the design of combinatorial assignment mechanism for two reasons. First, MVNNs are *universal* in the set of monotone and normalized value functions ([Weissteiner et al. 2022a](#), Theorem 1), i.e., any  $\hat{v}_i : \mathcal{X} \rightarrow \mathbb{R}_+$  that satisfies the following two properties can be represented *exactly* as a MVNN  $\mathcal{M}_i^\theta$ :

1. **Monotonicity (M)** (“additional items increase value”): For  $A, B \in 2^M$ : if  $A \subseteq B$  it holds that  $\hat{v}_i(A) \leq \hat{v}_i(B)$
2. **Normalization (N)** (“no value for empty bundle”):  $\hat{v}_i(\emptyset) = \hat{v}_i((0, \dots, 0)) := 0$ ,

Second, [Weissteiner et al. \(2022a\)](#) showed that an MVNN-based WDP, i.e.,  $\operatorname{argmax}_{a \in \mathcal{F}} \sum_{i \in N} \mathcal{M}_i^\theta(a_i)$ , can be succinctly

encoded as a MILP, which is key for the design of MVNN-based iterative combinatorial assignment mechanisms. Finally, [Weissteiner et al. \(2022a\)](#) experimentally showed that using MVNNs as  $\mathcal{A}_i$  in MLCA leads to SOTA performance.

## 2.4 NOMU

Recently, [Heiss et al. \(2022\)](#) introduced a novel method to estimate model uncertainty for NNs: *Neural optimization-based model uncertainty (NOMU)*. In contrast to other methods (e.g., ensembles), NOMU represents an *upper uncertainty bound (uUB)* as a *single and MILP-formalizable* NN. Thus, NOMU is particularly well suited for iterative combinatorial assignment, where uUB-based *winner determination problems (WDPs)* need to be solved hundreds of times to generate new informative queries. This, together with NOMU’s strong performance in noiseless BO, is the reason why we build on it and define a modified NOMU algorithm tailored to iterative combinatorial assignment (Section 3.1).

## 3 Bayesian Optimization-based ICA

In this section, we describe the design of our Bayesian Optimization-based Combinatorial Assignment (BOCA) mechanism. While the design is general, we here present it for the CA setting, leading to a BO-based ICA. The key idea is the following: Recall, that MLCA generates new value queries by solving the ML-based WDP  $q^{\text{new}} \in \operatorname{argmax}_{a \in \mathcal{F}} \sum_{i \in N} \mathcal{A}_i(a_i)$  (see Section 2.2). For the design of BOCA, we integrate a proper notion of uncertainty into MLCA by using an *upper uncertainty bound (uUB)* as the acquisition function  $\mathcal{A}_i$  (see Appendix C.1 for a review of

BO). To define our uUB and make it amenable to MLCA, we proceed in three steps: First, we combine MVNNs with a modified NOMU algorithm that is tailored to the characteristics of combinatorial assignment (Section 3.1). Second, we highlight the importance of proper parameter initialization for MVNNs and propose a more robust method (Section 3.2). Third, we present a more succinct MILP for MVNNs (Section 3.3). In the remainder of the paper, we make the following assumption:

**Assumption 1.** For all agents  $i \in N$ , the true and reported value functions  $v_i$  and  $\hat{v}_i$  fulfill the **Monotonicity (M)** and **Normalization (N)** property (see Section 2.3).

### 3.1 Model Uncertainty for Monotone NNs

We propose a modified NOMU architecture and loss that is specifically tailored to combinatorial assignment. Concretely, our algorithm is based on the following two key characteristics of combinatorial assignment: (i) since agents' value functions are monotonically increasing, the uUBs need to be monotonically increasing too, and (ii) due to the (finite) discrete input space, one can derive a closed-form expression of the 100%-uUB as an MVNN. Before we present our modified NOMU architecture and loss, we introduce the MVNN-based 100%-uUB.

Let  $\mathcal{H}$  denote a hypothesis class of functions  $f : X \rightarrow Y$  for some input and output spaces  $X$  and  $Y$  and let  $\mathcal{H}_{D^{\text{train}}} := \{f \in \mathcal{H} : f(x^{(l)}) = y^{(l)}, l = 1, \dots, n^{\text{train}}\}$  denote the set of all functions from  $\mathcal{H}$  that fit exactly through training points  $D^{\text{train}} = \{x^{(l)}, f(x^{(l)})\}_{l=1}^{n^{\text{train}}}$ . In the following, let

$$\mathcal{V} := \{\hat{v} : \mathcal{X} \rightarrow \mathbb{R}_+ \mid \text{satisfy (N) and (M)}\} \quad (5)$$

denote the set of all value functions that satisfy the *normalization* and *monotonicity* property. Next, we define the 100%-uUB.

**Definition 2** (100%-uUB). For a hypothesis class  $\mathcal{H}$  and a training set  $D^{\text{train}}$ , we define the 100%-uUB as  $f^{100\%-uUB}(x) := \sup_{f \in \mathcal{H}_{D^{\text{train}}}} f(x)$  for every  $x \in X$ .

In Theorem 1, we show that for  $\mathcal{H} = \mathcal{V}$  the 100%-uUB can be explicitly represented as an MVNN.

**Theorem 1** (MVNN-based 100%-uUB). Let  $((1, \dots, 1), \hat{v}_i((1, \dots, 1))) \in D^{\text{train}}$ . Then for  $\mathcal{H} = \mathcal{V}$  it holds that  $f^{100\%-uUB}(x) = \max_{f \in \mathcal{V}_{D^{\text{train}}}} f(x)$  for all  $x \in \mathcal{X}$  and  $f^{100\%-uUB} \in \mathcal{V}_{D^{\text{train}}}$  can be represented as a two hidden layer MVNN with  $n^{\text{train}}$  neurons per layer, which we will denote as  $\mathcal{M}_i^{100\%-uUB}$  going forward.<sup>1</sup>

*Proof.* We prove Theorem 1 in Appendix D.1, following a similar idea as the universality proof in (Weissteiner et al. 2022a, Theorem 1).  $\square$

Using the MVNN-based 100%-uUB  $\mathcal{M}_i^{100\%-uUB}$ , we can now define our modified NOMU architecture and loss.

<sup>1</sup> $\mathcal{M}_i^{100\%-uUB}(\cdot)$  depends on a training set  $D^{\text{train}}$ , i.e., rigorously  $\mathcal{M}_i^{100\%-uUB}[D^{\text{train}}](\cdot)$ , which we drop in our notation for brevity.

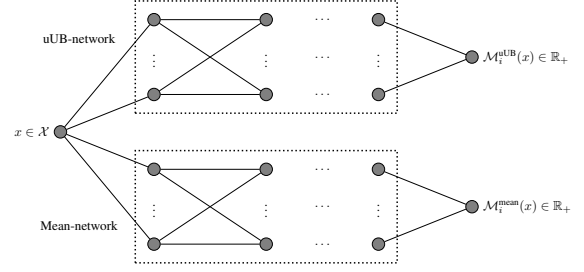


Figure 1:  $\mathcal{M}_i^{\text{NOMU}}$ : a modification of NOMU's original architecture for the combinatorial assignment domain

**The Architecture.** Towards defining the architecture, we first observe that if the true function is monotonically increasing, the corresponding uUB needs to be monotonically increasing as well (Propositions 1 and 2 in Appendix D.2). Given that bidders' value functions are monotone (Assumption 1), this implies that our uUB must also be monotonically increasing. Thus, instead of the original NOMU architecture that outputs the (raw) uncertainty (i.e., an estimate of the posterior standard deviation) which is *not* monotone, we can modify NOMU's architecture and directly output the monotone uUB. Given this, we propose the following architecture  $\mathcal{M}_i^{\text{NOMU}}$  to estimate the uUB for bidder  $i \in N$ .  $\mathcal{M}_i^{\text{NOMU}}$  consists of two sub-MVNNs with two outputs: the mean prediction  $\mathcal{M}_i^{\text{mean}} : \mathcal{X} \rightarrow \mathbb{R}$  and the estimated uUB  $\mathcal{M}_i^{\text{uUB}} : \mathcal{X} \rightarrow \mathbb{R}$ . In Figure 1, we provide a schematic representation of  $\mathcal{M}_i^{\text{NOMU}}$  (see Appendix D.2 for details).

**The Loss.** Next, we formulate a new NOMU loss function  $L^\pi$  tailored to combinatorial assignment. Since we have a closed-form expression of the 100%-uUB as MVNN  $\mathcal{M}_i^{100\%-uUB}$  (Theorem 1), we are able to enforce that  $\mathcal{M}_i^{\text{mean}} \leq \mathcal{M}_i^{\text{uUB}} \leq \mathcal{M}_i^{100\%-uUB}$  via the design of our new loss function. Let  $\mathcal{M}_i^{\text{mean}}$  be a trained mean-MVNN with a standard loss, (e.g. MAE). We train  $\mathcal{M}_i^{\text{uUB}}$  with loss  $L^\pi$  and L2-regularization parameter  $\lambda > 0$ , i.e., minimizing  $L^\pi(\mathcal{M}_i^{\text{uUB}}) + \lambda \|\theta\|_2^2$  via gradient descent.

**Definition 3** (NOMU Loss Tailored to Combinatorial Assignment). Let  $\pi = (\pi_{sq}, \pi_{exp}, c_{exp}, \bar{\pi}, \underline{\pi}) \in \mathbb{R}_+^5$  be a tuple of hyperparameters. For a training set  $D^{\text{train}}$ ,  $L^\pi$  is defined as<sup>2</sup>

$$L^\pi(\mathcal{M}_i^{\text{uUB}}) := \pi_{sq} \sum_{l=1}^{n^{\text{train}}} L_1^\beta(\mathcal{M}_i^{\text{uUB}}(x^{(l)}), y^{(l)}) \quad (6a)$$

$$+ \pi_{exp} \int_{[0,1]^m} u(-c_{exp}(\min\{\mathcal{M}_i^{\text{uUB}}(x), \mathcal{M}_i^{100\%-uUB}(x)\} - \mathcal{M}_i^{\text{mean}}(x))) dx \quad (6b)$$

$$+ \pi_{exp} c_{exp} \bar{\pi} \int_{[0,1]^m} L_1^\beta((\mathcal{M}_i^{\text{uUB}}(x) - \mathcal{M}_i^{100\%-uUB}(x))^+) dx \quad (6c)$$

$$+ \pi_{exp} c_{exp} \underline{\pi} \int_{[0,1]^m} L_1^\beta((\mathcal{M}_i^{\text{mean}}(x) - \mathcal{M}_i^{\text{uUB}}(x))^+) dx \quad (6d)$$

where  $L_1^\beta$  is the smooth L1-loss with threshold  $\beta$  (see Definition D.1),  $(\cdot)^+$  the positive part, and  $u := 1 + \text{ELU}$  is convex

<sup>2</sup>See Definition D.3 for the detailed loss.

monotonically increasing with ELU being exponential linear unit (ELU) (see Definition D.2).

The interpretations of the four terms are as follows:

- (6a) enforces that  $\mathcal{M}_i^{\text{uUB}}$  fits through the training data.
- (6b) pushes  $\mathcal{M}_i^{\text{uUB}}$  up as long as it is below the 100%-uUB  $\mathcal{M}_i^{100\%-\text{uUB}}$ . This force gets weaker the further  $\mathcal{M}_i^{\text{uUB}}$  is above the mean  $\mathcal{M}_i^{\text{mean}}$  (especially if  $c_{\text{exp}}$  is large).  $\pi_{\text{exp}}$  controls the overall strength of (6b) and  $c_{\text{exp}}$  controls how fast this force increases when  $\mathcal{M}_i^{\text{uUB}} \rightarrow \mathcal{M}_i^{\text{mean}}$ . Thus, increasing  $\pi_{\text{exp}}$  increases the uUB and increasing  $c_{\text{exp}}$  increases the uUBs in regions where it is close to  $\mathcal{M}_i^{\text{mean}}$ . Weakening (6b) (i.e.,  $\pi_{\text{exp}} c_{\text{exp}} \rightarrow 0$ ) leads to  $\mathcal{M}_i^{\text{uUB}} \approx \mathcal{M}_i^{\text{mean}}$ . Strengthening (6b) by increasing  $\pi_{\text{exp}} c_{\text{exp}}$  in relation to regularization<sup>3</sup> leads to  $\mathcal{M}_i^{\text{uUB}} \approx \mathcal{M}_i^{100\%-\text{uUB}}$ .
- (6c) enforces that  $\mathcal{M}_i^{\text{uUB}} \leq \mathcal{M}_i^{100\%-\text{uUB}}$ . The strength of this term is determined by  $\bar{\pi} \cdot (\pi_{\text{exp}} c_{\text{exp}})$ , where  $\bar{\pi}$  is the (6c)-specific hyperparameter and  $\pi_{\text{exp}} c_{\text{exp}}$  adjusts the strength of (6c) to (6b).
- (6d) enforces  $\mathcal{M}_i^{\text{uUB}} \geq \mathcal{M}_i^{\text{mean}}$ . The interpretation of  $\bar{\pi}$  and  $\pi_{\text{exp}} c_{\text{exp}}$  is analogous to (6c).

As in (Heiss et al. 2022), in the implementation of  $L^\pi$ , we approximate Equations (6b) to (6d) via Monte Carlo integration using additional, *artificial input points*  $D^{\text{art}} := \{x^{(l)}\}_{l=1}^{n^{\text{art}}} \overset{i.i.d.}{\sim} \text{Unif}([0, 1]^m)$ .

**Figure 2.** In Figure 2, we present a visualization of the output of  $\mathcal{M}_i^{\text{NOMU}}$  (i.e.,  $\mathcal{M}_i^{\text{mean}}$  and  $\mathcal{M}_i^{\text{uUB}}$ ) and  $\mathcal{M}_i^{100\%-\text{uUB}}$  for the national bidder in the LSVM domain of the spectrum auction test suite (SATS) (Weiss, Lubin, and Seuken 2017). In noiseless regression, uncertainty should vanish at observed training points, but (model) uncertainty should remain about value predictions for bundles that are very different from the bundles observed in training. Figure 2 shows that our uUB  $\mathcal{M}_i^{\text{uUB}}$  nicely fulfills this. Moreover, we have shown in Appendix D.2 that  $\mathcal{M}_i^{\text{uUB}}$  is monotonically increasing, since we assume that value functions fulfill the monotonicity property. This implies that once we observe a value for the full bundle, we obtain a globally bounded 100%-uUB, i.e., see  $\mathcal{M}_i^{100\%-\text{uUB}}$  in Figure 2. Furthermore, we see that  $\mathcal{M}_i^{100\%-\text{uUB}}$  jumps to a high value when only a single item is added to an already queried bundle, but then often stays constant (e.g.  $|x| = 12, \dots, 18$  in Figure 2). Thus, using such a 100%-uUB as acquisition function, MLCA would only add a single item to an already queried bundle to have more items left for the other bidders instead of properly exploring the bundle space. Our uUB  $\mathcal{M}_i^{\text{uUB}}$  circumvents this via implicit and explicit regularization and yields a useful uUB.

### 3.2 Parameter Initialization for MVNNs

We now discuss how to properly initialize parameters for MVNNs. Importantly, note that our proposed acquisition function, i.e., the *MVNN-based uUB*  $\mathcal{M}_i^{\text{uUB}}$ , is an MVNN. As we will show next, to achieve the best performance of

<sup>3</sup>Regularization can be early stopping or a small number of neurons (implicit) or L2-regularization on the parameters (explicit).

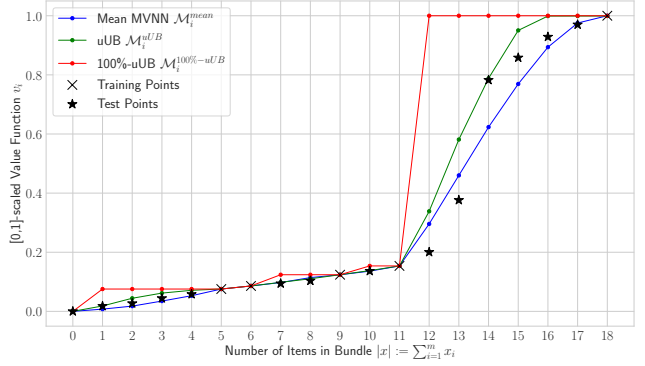


Figure 2:  $\mathcal{M}_i^{\text{mean}}$ ,  $\mathcal{M}_i^{\text{uUB}}$  and  $\mathcal{M}_i^{100\%-\text{uUB}}$  along an increasing 1D subset-path (i.e., for all bundles  $x^{(j)}, x^{(k)}$  on the x-axis it holds that for  $j \leq k : x^{(j)} \subset x^{(k)}$ ).

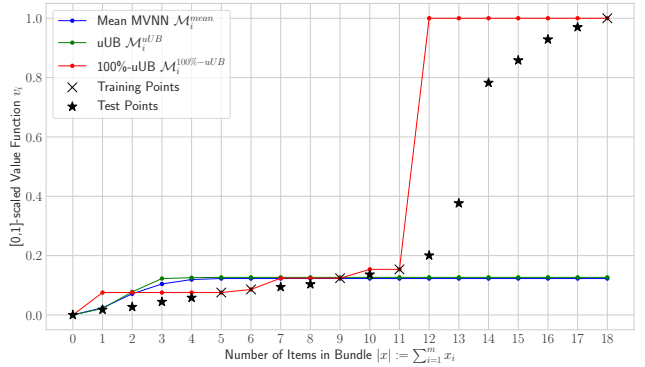


Figure 3: In contrast to our proposed initialization (see Figure 2), training fails with generic initialization already for relatively small [64,64]-architectures that were used here.

BOCA (in fact of any MVNN training), an adjusted, non-generic parameter initialization is very important.

**Generic Initialization.** For standard NNs, it is most common to use a weight initialization with zero mean  $\mu_k := \mathbb{E}[W_{j,l}^{i,k}] = 0$  and non-zero variance  $\sigma_k^2 := \mathbb{V}[W_{j,l}^{i,k}] \neq 0$ . Then the mean of each pre-activated neuron of the first hidden layer is zero and the variance  $\mathbb{V}[(W^{i,1}x)_j] = d^{i,0} \sigma_1^2 \bar{x}^2$ , if  $(W_{j,l}^{i,1})_{l=1}^{d^{i,0}}$  are i.i.d., where  $\bar{x}^2 = \frac{1}{d^{i,0}} \sum_{l=1}^{d^{i,0}} x_l^2$ .<sup>4</sup> Analogously, one can compute the *conditional* mean and the *conditional* variance of a pre-activated neuron in any layer  $k$  by replacing  $x$  by the output  $z^{i,k-1}$  of the previous layer, i.e.  $\mathbb{E}[(W^{i,k} z^{i,k-1})_j | z^{i,k-1}] = 0$  and  $\mathbb{V}[(W^{i,k} z^{i,k-1})_j | z^{i,k-1}] = d^{i,0} \sigma_1^2 (z^{i,k-1})^2$ . For  $\sigma_k \propto \frac{1}{\sqrt{d^{i,k-1}}}$ , the conditional mean and variance does not depend on the dimensions  $d^{i,k}$  of the layers, which is why

<sup>4</sup>We assume that the biases  $b^{i,k} = 0$  are all initialized to zero throughout Section 3.2 to keep the notation simpler, while we formulate everything for the general case including random biases in Appendix E and in our code.

generic initialization methods scale the initial distribution by  $s_k \propto \frac{1}{\sqrt{d^{i,k-1}}}$ .

**Problem.** Unfortunately, this generic initialization approach can dramatically fail for MVNNs: For any non-zero initialization, the non-negativity constraint of the weights implies that the mean  $\mu_k > 0$ . This implies that the mean of a pre-activated neuron in the first hidden layer is  $\mathbb{E}[(W^{i,1}x)_j] = d^{i,0}\mu_1\bar{x}$ . For a generic scaling  $s_k$  one would obtain  $\mu_k \propto \frac{1}{\sqrt{d^{i,k-1}}}$  and thus the mean  $\mathbb{E}[(W^{i,1}x)_j] \propto d^{i,0}\frac{1}{\sqrt{d^{i,0}}}\bar{x} = \sqrt{d^{i,0}}\bar{x}$  of the preactivated neurons diverges to infinity with a rate of  $\sqrt{d^{i,0}}$  as  $d^{i,0} \rightarrow \infty$ . Analogously, the pre-activated neurons of every layer diverge to infinity as  $d^{i,k-1} \rightarrow \infty$ . This is particularly problematic for bReLU (as used in MVNNs) as their gradient is zero on  $[0, t^{i,k}]^c$ . Figure 3 shows that both MVNNs  $\mathcal{M}_i^{\text{mean}}$  and  $\mathcal{M}_i^{\text{uUB}}$  get “stuck.” This happens because already at initialization, every neuron in the first hidden layer has a pre-activation that is larger than  $t^{i,1}$  for every training point.

This could be solved by scaling down the initial weights even more, e.g.,  $W_{j,l}^{i,k} \sim \text{Unif}[0, \frac{2}{d^{i,k-1}}]$  resulting in  $\mu_k = \frac{1}{d^{i,k-1}}$ . However, this induces a new problem of vanishing conditional variance  $\mathbb{V}[(W^{i,k}z^{i,k-1})_j | z^{i,k-1}]$  with a rate of  $\mathcal{O}(\frac{1}{d^{i,k-1}})$  for wide (i.e.,  $d^{i,k-1}$  large) MVNNs. Overall, it is impossible to simultaneously solve both problems by just scaling the distribution by a factor  $s_k$ , because the conditional mean  $\mathbb{E}[(W^{i,k}z^{i,k-1})_j | z^{i,k-1}]$  scales with  $s_k \cdot d^{i,k-1}$  and the conditional variance  $\mathbb{V}[(W^{i,k}z^{i,k-1})_j | z^{i,k-1}]$  scales with  $s_k^2 \cdot d^{i,k-1}$ . Thus, for wide MVNNs, one of those two problems (i.e., either diverging expectation or vanishing variance) would persist.

**Solution.** We introduce a new initialization method that solves *both* problems at the same time. For this, we propose an i.i.d. mixture distribution of two different uniform distributions. For each weight, with probability  $(1 - p_k)$  we sample from  $\text{Unif}[0, A_k]$ , and with probability  $p_k$  we sample from  $\text{Unif}[0, B_k]$ . If we choose  $p_k$  and  $A_k$  small enough, we can get arbitrarily small  $\mu_k$  while not reducing  $\sigma_k$  too much. In Appendix E, we provide formulas for how to choose  $A_k$ ,  $B_k$  and  $p_k$  depending on  $d^{i,k-1}$ . In Theorem 3 in Appendix E, we prove that, if the parameters are chosen in this way, then the conditional mean and conditional variance do not explode or vanish with increasing  $d^{i,k-1}$  but stay constant for large  $d^{i,k-1}$ . Note that, in Figure 2, for  $\mathcal{M}_i^{\text{mean}}$  and  $\mathcal{M}_i^{\text{uUB}}$ , we used our proposed initialization method for suitable  $A_k$ ,  $B_k$  and  $p_k$ , such that the problem induced by a generic initialization from Figure 3 is resolved.

### 3.3 Mixed Integer Linear Program (MILP)

A key step in ML-powered iterative combinatorial assignment mechanisms is finding the social welfare-maximizing allocation, i.e., solving the *ML-based winner determination problem* (ML-WDP). Thus, a key requirement posed on any

acquisition function  $\mathcal{A}_i^\theta$  (including an uUB) in such a mechanism is to be able to efficiently solve

$$\max_{a \in \mathcal{F}} \sum_{i \in N} \mathcal{A}_i^\theta(a_i). \quad (7)$$

Weissteiner et al. (2022a) proposed a MILP for MVNNs, i.e.,  $\mathcal{A}_i^\theta := \mathcal{M}_i^\theta$ , to efficiently solve eq. (7). Their MILP was based on a reformulation of the  $\min(\cdot, \cdot)$  and  $\max(\cdot, \cdot)$  in the bReLU activation  $\min(\max(\cdot, 0), t)$ . Thus, it required twice the number of binary variables *and* linear constraints as for a plain ReLU-NN. Since we use an MVNN-based uUB  $\mathcal{A}_i^\theta := \mathcal{M}_i^{\text{uUB}}$  as the acquisition function, we could directly use their MILP formulation. However, instead, we propose a new MILP, which is significantly more succinct. For this, let  $o^{i,k} := W^{i,k}z^{i,k-1} + b^{i,k}$  be the *pre-activated* output and  $z^{i,k} := \varphi_{0,t^{i,k}}(o^{i,k})$  be the output of the  $k^{\text{th}}$  layer with  $l^{i,k} \leq o^{i,k} \leq u^{i,k}$ , where the tight lower (upper) bound  $l^{i,k}$  ( $u^{i,k}$ ) is derived by forward-propagating the empty (full) bundle (Weissteiner et al. 2022a, Fact 1). In Theorem 2, we state our new MILP (see Appendix F.1 for its proof).<sup>5</sup>

**Theorem 2** (MVNN MILP Tailored to Combinatorial Assignment). *Let  $\mathcal{A}_i^\theta = \mathcal{M}_i^{\text{uUB}}$  be our MVNN-based uUB acquisition function. The ML-based WDP (7) can be formulated as the following MILP:*

$$\begin{aligned} & \max_{a \in \mathcal{F}, z^{i,k}, \alpha^{i,k}, \beta^{i,k}} \left\{ \sum_{i \in N} W^{i,K_i} z^{i,K_i-1} \right\} & (8) \\ & \text{s.t. for } i \in N \text{ and } k \in \{1, \dots, K_i - 1\} \\ & z^{i,0} = a_i & (9) \\ & z^{i,k} \leq \alpha^{i,k} \cdot t^{i,k} & (10) \\ & z^{i,k} \leq o^{i,k} - l^{i,k} \cdot (1 - \alpha^{i,k}) & (11) \\ & z^{i,k} \geq \beta^{i,k} \cdot t^{i,k} & (12) \\ & z^{i,k} \geq o^{i,k} + (t^{i,k} - u) \beta^{i,k} & (13) \\ & \alpha^{i,k} \in \{0, 1\}^{d^{i,k}}, \beta^{i,k} \in \{0, 1\}^{d^{i,k}} & (14) \end{aligned}$$

Note that for each neuron of  $\mathcal{A}_i^\theta = \mathcal{M}_i^{\text{uUB}}$ , our new MILP has only 4 linear constraints, i.e., respective components of eqs. (10) to (13), compared to 8 in (Weissteiner et al. 2022a). Moreover, in contrast to the MILP in (Weissteiner et al. 2022a), our MILP does not make use of any “big-M” constraints, which are known to be numerically unstable.

## 4 Experiments

In this section, we experimentally evaluate the performance of BOCA in the CA domain. To this end, we equip the MLCA mechanism (see Section 2.2) with our new acquisition function  $\mathcal{A}_i = \mathcal{M}_i^{\text{uUB}}$  to estimate bidders’ preferences. We compare the efficiency of BOCA against the previously proposed MVNN-based and NN-based MLCA from (Weissteiner et al. 2022a) which do not make use of any notion of uncertainty. We use our new parameter initialization method (Section 3.2) for  $\mathcal{M}_i^{\text{uUB}}$ , and we use our new MILP (Theorem 2) for solving the corresponding WDPs.

<sup>5</sup>All vector inequalities should be understood component-wise.

DOMAIN	$Q^{\max}$	EFFICIENCY LOSS IN % ↓					T-TEST FOR EFFICIENCY:	
		BOCA	WEISSTEINER ET AL. (2022A) MVNN-MLCA	WEISSTEINER AND SEUKEN (2020) NN-MLCA	WEISSTEINER ET AL. (2022B) FT-MLCA	RS	$\mathcal{H}_0 : \mu_{\text{MVNN-MLCA}} \leq \mu_{\text{BOCA}}$	$\mathcal{H}_0 : \mu_{\text{NN-MLCA}} \leq \mu_{\text{BOCA}}$
LSVM	100	0.39 ± 0.30	00.70 ± 0.40	02.91 ± 1.44	01.54 ± 0.65	31.73 ± 2.15	$p_{\text{VAL}} = 9\text{e-}2$	$p_{\text{VAL}} = 3\text{e-}4$
SRVM	100	0.06 ± 0.02	00.23 ± 0.06	01.13 ± 0.22	00.72 ± 0.16	28.56 ± 1.74	$p_{\text{VAL}} = 5\text{e-}6$	$p_{\text{VAL}} = 2\text{e-}13$
MRVM	100	7.77 ± 0.34	08.16 ± 0.41	09.05 ± 0.53	10.37 ± 0.57	48.79 ± 1.13	$p_{\text{VAL}} = 8\text{e-}2$	$p_{\text{VAL}} = 2\text{e-}5$

Table 1: BOCA vs MVNN-MLCA, NN-MLCA, Fourier transform (FT)-MLCA and random search (RS). Shown are averages and a 95% CI on a test set of 50 instances. Winners based on a t-test with significance level of 1% are marked in grey.

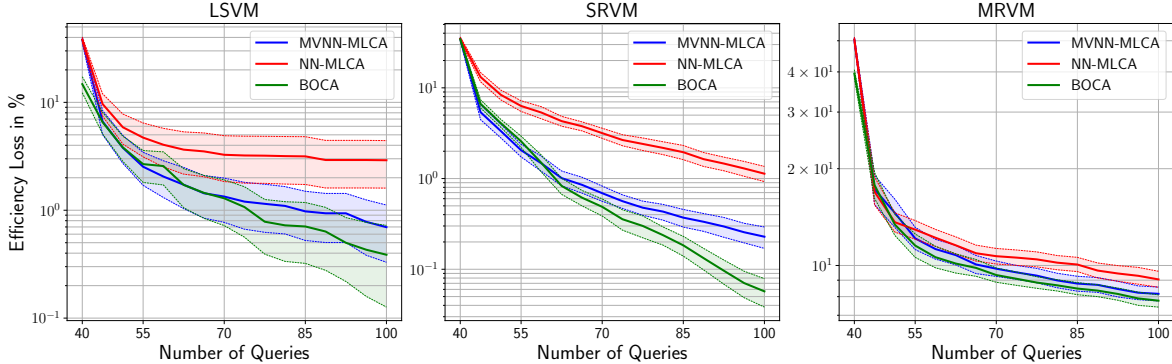


Figure 4: Efficiency loss paths (i.e., regret plots) of BOCA compared to the results from Weissteiner et al. (2022a) of MVNN-MLCA and NN-MLCA without any notion of uncertainty. Shown are averages with 95% CIs over 50 CA instances.

**Experiment Setup.** To generate synthetic CA instances, we use the following three domains from the spectrum auction test suite (SATS) (Weiss, Lubin, and Seuken 2017): LSVM, SRVM, and MRVM (see Appendix G.1 for details).<sup>6</sup> SATS gives us access to the true optimal allocation  $a^*$ , which we use to measure the *efficiency loss*, i.e.,  $1 - V(a_R^*)/V(a^*)$  when eliciting reports  $R$  via MLCA. We report efficiency loss (and not revenue), as spectrum auctions are government-run, with a mandate to maximize welfare (Cramton 2013). For each domain, we use  $Q^{\text{init}} = 40$  initial random queries (including the full bundle for the calculation of  $\mathcal{M}_i^{100\%-\text{uUB}}$ ) and set the query budget to  $Q^{\max} = 100$ . We terminate any mechanisms in an intermediate iteration if it already found an allocation with 0% efficiency loss.

**Hyperparameter Optimization (HPO).** We use *random search* (RS) (Bergstra and Bengio 2012) to optimize the hyperparameters of the mean MVNN  $\mathcal{M}_i^{\text{mean}}$  and of our MVNN-based uUB  $\mathcal{M}_i^{\text{uUB}}$ . The HPO includes the NN-architecture parameters, training parameters such as learning rate, NOMU parameters, and initialization parameters (see Section 3.2). RS was carried out independently for each bidder type and SATS domain with a budget of 500 configurations, where each configuration was evaluated on 100 SATS instances. For each instance, the MVNNs  $\mathcal{M}_i^{\text{mean}}$  and  $\mathcal{M}_i^{\text{uUB}}$  were trained on uniformly at random chosen bundle-value pairs  $D^{\text{train}}$  and evaluated on a disjoint test set of different bundle-value pairs  $D^{\text{test}}$ . To select the winner configuration, we consider as evaluation metric the quantile-loss on the test set and the MAE on the training set, i.e., for each configura-

tion and instance we calculate

$$|D^{\text{test}}|^{-1} \sum_{(x,y) \in D^{\text{test}}} \max\{(y - \mathcal{M}_i^{\text{uUB}}(x))q, (\mathcal{M}_i^{\text{uUB}}(x) - y)(1 - q)\} + \text{MAE}(D^{\text{train}}), \quad (15)$$

which we then average over all 100 instances. We used four quantile parameters  $q \in \{0.6, 0.75, 0.9, 0.95\}$  in eq. (15) to achieve different levels of exploration (i.e., the resulting uUBs are larger the larger the  $q$  in eq. (15)). This evaluation metric *simultaneously* measures the quality of the uUB on the test data (via the first term, i.e., the  $q$ -loss) as well as the quality of the uUB predictions on the training data (via the second term, i.e., the MAE). For each quantile  $q$  and SATS domain, we then proceed with the winner configuration of  $\mathcal{M}_i^{\text{uUB}}$  and evaluate the efficiency of BOCA on a separate set of 50 instances. Details on hyperparameter ranges and the training procedure are provided in Appendices G.2 to G.3.

**Results.** In Table 1, we show the average efficiency loss of each approach after  $Q^{\max} = 100$  queries (see Appendix G.4 for more detailed results). We observe that our proposed BOCA outperforms MVNN-based MLCA (MVNN-MLCA) on the SRVM domain in a statistically significant way, and it performs on-par in LSVM and MRVM, with a slightly better average performance. Given that MVNNs previously achieved SOTA performance, we also outperform the other benchmarks (i.e., NN and FT-MLCA). The poor performance of RS highlights the intrinsic difficulty of this task. Note that the amount of exploration needed is domain dependent, which explains why BOCA outperforms MVNN-MLCA in some but not all domains. However, our results also show that using a uUB (as in BOCA) instead of just a mean prediction (as in MVNN-MLCA) does not hurt.

Figure 4 shows the efficiency loss path for all domains. This shows that the superior (avg) performance of  $\mathcal{M}_i^{\text{uUB}}$  does not only hold at the end of the auction (at  $Q^{\max} = 100$ ),

<sup>6</sup>We do not use GSVM, as Weissteiner et al. (2022a) already achieved 0% efficiency loss in GSVM via MVNN-based MLCA.

but also for a large range of queries: in LSVM, BOCA is better (on avg) for [70,100]; in SRVM, BOCA is significantly better for [70,100]; in MRVM, BOCA is better (on avg) for [0,100] (see Appendix G.5 for more details).

## 5 Conclusion

In this paper, we have proposed a Bayesian Optimization-based Combinatorial Assignment (BOCA) mechanism. On a conceptual level, our main contribution is the integration of model uncertainty over agents' preferences into ML-based preference elicitation. On a technical level, we have designed a new method for estimating an upper uncertainty bound that exploits the monotonicity of agents' preferences in the combinatorial assignment domain and the finite nature of this setting. Our experiments have shown that BOCA achieves efficiency that is as good or higher than the SOTA. An interesting direction for future work is the evaluation of BOCA in other combinatorial assignment domains, such as course allocation or combinatorial exchanges.

## Acknowledgments

This paper is part of a project that has received funding from the European Research Council (ERC) under the European Union's Horizon 2020 research and innovation program (Grant agreement No. 805542).

## References

Ausubel, L.; and Cramton, P. 2011. Auction design for wind rights. *Report to Bureau of Ocean Energy Management, Regulation and Enforcement*. 1

Ausubel, L. M.; and Baranov, O. 2017. A practical guide to the combinatorial clock auction. *Economic Journal*, 127(605): F334–F350. 1, 22

Ausubel, L. M.; Cramton, P.; and Milgrom, P. 2006. The clock-proxy auction: A practical combinatorial auction design. In Cramton, P.; Shoham, Y.; and Steinberg, R., eds., *Combinatorial Auctions*, 115–138. MIT Press. 1

Bergstra, J.; and Bengio, Y. 2012. Random search for hyperparameter optimization. *Journal of machine learning research*, 13(2). 7

Bichler, M.; Fux, V.; and Goeree, J. K. 2019. Designing combinatorial exchanges for the reallocation of resource rights. *Proceedings of the National Academy of Sciences*, 116(3): 786–791. 1

Blundell, C.; Cornebise, J.; Kavukcuoglu, K.; and Wierstra, D. 2015. Weight uncertainty in neural networks. In *32nd International Conference on Machine Learning (ICML)*. 2

Bonilla, E. V.; Guo, S.; and Sanner, S. 2010. Gaussian process preference elicitation. *Advances in neural information processing systems*, 23. 2

Brero, G.; Lubin, B.; and Seuken, S. 2018. Combinatorial Auctions via Machine Learning-based Preference Elicitation. In *Proceedings of the 27th International Joint Conference on Artificial Intelligence*. 1

Brero, G.; Lubin, B.; and Seuken, S. 2021. Machine Learning-powered Iterative Combinatorial Auctions. *arXiv preprint arXiv:1911.08042*. 1, 2, 3, 10, 11

Budish, E. 2011. The combinatorial assignment problem: Approximate competitive equilibrium from equal incomes. *Journal of Political Economy*, 119(6): 1061–1103. 1

Cramton, P. 2013. Spectrum auction design. *Review of Industrial Organization*, 42(2): 161–190. 1, 7

De Ath, G.; Everson, R. M.; Rahat, A. A.; and Fieldsend, J. E. 2021. Greed is good: Exploration and exploitation trade-offs in Bayesian optimisation. *ACM Transactions on Evolutionary Learning and Optimization*, 1(1): 1–22. 22

Frazier, P. I. 2018. A tutorial on Bayesian optimization. *arXiv preprint arXiv:1807.02811*. 11

Gal, Y.; and Ghahramani, Z. 2016. Dropout as a Bayesian Approximation: Representing Model Uncertainty in Deep Learning. In *33rd International Conference on Machine Learning (ICML)*, 1050–1059. 2, 14

Goeree, J. K.; and Holt, C. A. 2010. Hierarchical package bidding: A paper & pencil combinatorial auction. *Games and Economic Behavior*, 70(1): 146–169. 20

Graves, A. 2011. Practical variational inference for neural networks. In *Advances in neural information processing systems*, 2348–2356. 2

Heiss, J.; Weissteiner, J.; Wutte, H.; Seuken, S.; and Teichmann, J. 2022. NOMU: Neural Optimization-based Model Uncertainty. In *Proceedings of the 39th International Conference on Machine Learning (ICML)*. 2, 3, 5, 12, 13, 14, 15, 20

Hernández-Lobato, J. M.; and Adams, R. 2015. Probabilistic backpropagation for scalable learning of bayesian neural networks. In *International Conference on Machine Learning*, 1861–1869. 2

Kuleshov, V.; Fenner, N.; and Ermon, S. 2018. Accurate Uncertainties for Deep Learning Using Calibrated Regression. In *Proceedings of the 35th International Conference on Machine Learning*, 2796–2804. PMLR. 14

Lakshminarayanan, B.; Pritzel, A.; and Blundell, C. 2017. Simple and scalable predictive uncertainty estimation using deep ensembles. In *Advances in neural information processing systems*, 6402–6413. 2, 14

Nisan, N.; and Segal, I. 2006. The communication requirements of efficient allocations and supporting prices. *Journal of Economic Theory*, 129(1): 192–224. 1

Ober, S. W.; and Rasmussen, C. E. 2019. Benchmarking the neural linear model for regression. *arXiv preprint arXiv:1912.08416*. 2

Papalexopoulos, P.; Tjandraatmadja, C.; Anderson, R.; Vielma, J. P.; and Belanger, D. 2022. Constrained Discrete Black-Box Optimization using Mixed-Integer Programming. In *Proceedings of the 39th International Conference on Machine Learning*, 17295–17322. PMLR. 12

Sandholm, T.; and Boutilier, C. 2006. Preference elicitation in combinatorial auctions. *Combinatorial auctions*, 10. 1

Scheffel, T.; Ziegler, G.; and Bichler, M. 2012. On the impact of package selection in combinatorial auctions: an experimental study in the context of spectrum auction design. *Experimental Economics*, 15(4): 667–692. 20



- Srinivas, N.; Krause, A.; Kakade, S. M.; and Seeger, M. W. 2012. Information-Theoretic Regret Bounds for Gaussian Process Optimization in the Bandit Setting. *IEEE Transactions on Information Theory*, 58(5): 3250–3265. [11](#)
- Weiss, M.; Lubin, B.; and Seuken, S. 2017. Sats: A universal spectrum auction test suite. In *Proceedings of the 16th Conference on Autonomous Agents and MultiAgent Systems*, 51–59. [5](#), [7](#), [20](#)
- Weissteiner, J.; Heiss, J.; Siems, J.; and Seuken, S. 2022a. Monotone-Value Neural Networks: Exploiting Preference Monotonicity in Combinatorial Assignment. In *Proceedings of the 31st International Joint Conference on Artificial Intelligence*. [2](#), [3](#), [4](#), [6](#), [7](#), [12](#), [18](#), [19](#), [20](#), [22](#)
- Weissteiner, J.; and Seuken, S. 2020. Deep Learning-powered Iterative Combinatorial Auctions. In *Proceedings of the 34th AAAI Conference of Artificial Intelligence*, 2284–2293. [2](#), [7](#), [12](#)
- Weissteiner, J.; Wendler, C.; Seuken, S.; Lubin, B.; and Püschel, M. 2022b. Fourier Analysis-based Iterative Combinatorial Auctions. In *Proceedings of the 31st International Joint Conference on Artificial Intelligence*. [2](#), [7](#)
- Wenzel, F.; Snoek, J.; Tran, D.; and Jenatton, R. 2020. Hyperparameter ensembles for robustness and uncertainty quantification. *arXiv preprint arXiv:2006.13570*. [2](#)

# Appendix

## Bayesian Optimization-based Combinatorial Assignment

### A A Machine Learning-powered ICA

In this section, we present in detail the *machine learning-powered combinatorial auction (MLCA)* by Brero, Lubin, and Seuken (2021).

At the core of MLCA is a *query module* (Algorithm 1), which, for each bidder  $i \in I \subseteq N$ , determines a new value query  $q_i$ . First, in the *estimation step* (Line 1), an ML algorithm  $\mathcal{A}_i$  is used to learn bidder  $i$ 's valuation from reports  $R_i$ . Next, in the *optimization step* (Line 2), an *ML-based WDP* is solved to find a candidate  $q$  of value queries. In principle, any ML algorithm  $\mathcal{A}_i$  that allows for solving the corresponding ML-based WDP in a fast way could be used. Finally, if  $q_i$  has already been queried before (Line 4), another, more restricted ML-based WDP (Line 6) is solved and  $q_i$  is updated correspondingly. This ensures that all final queries  $q$  are new.

**Algorithm 1:** NEXTQUERIES( $I, R$ ) (Brero et al. 2021)

---

**Inputs:** Index set of bidders  $I$  and reported values  $R$

```

1 foreach  $i \in I$  do Fit  $\mathcal{A}_i$  on  $R_i$ :  $\mathcal{A}_i[R_i]$   $\triangleright$  Estimation step
2 Solve  $q \in \operatorname{argmax}_{a \in \mathcal{F}} \sum_{i \in I} \mathcal{A}_i[R_i](a_i)$   $\triangleright$  Optimization step
3 foreach  $i \in I$  do
4   if  $(q_i, \hat{v}_i(q_i)) \in R_i$  then  $\triangleright$  Bundle already queried
5     Define  $\mathcal{F}' = \{a \in \mathcal{F} : a_i \neq x, \forall (x, \hat{v}_i(x)) \in R_i\}$ 
6     Re-solve  $q' \in \operatorname{argmax}_{a \in \mathcal{F}'} \sum_{l \in I} \mathcal{A}_l[R_l](a_l)$ 
7     Update  $q_i = q'_i$ 
8   end
9 end
10 return Profile of new queries  $q = (q_1, \dots, q_n)$ 

```

---

In Algorithm 2, we present MLCA. In the following, let  $R_{-i} = (R_1, \dots, R_{i-1}, R_{i+1}, \dots, R_n)$ . MLCA proceeds in rounds until a maximum number of queries per bidder  $Q^{\max}$  is reached. In each round, it calls Algorithm 1 ( $Q^{\text{round}} - 1$ ) $n + 1$  times: for each bidder  $i \in N$ ,  $Q^{\text{round}} - 1$  times excluding a different bidder  $j \neq i$  (Lines 5–10, sampled *marginal economies*) and once including all bidders (Line 11, *main economy*). In total each bidder is queried  $Q^{\text{round}}$  bundles per round in MLCA. At the end of each round, the mechanism receives reports  $R^{\text{new}}$  from all bidders for the newly generated queries  $q^{\text{new}}$  and updates the overall elicited reports  $R$  (Lines 12–14). In Lines 16–17, MLCA computes an allocation  $a_R^*$  that maximizes the *reported* social welfare (see Equation (1)) and determines VCG payments  $p(R)$  based on the reported values  $R$  (see Appendix Definition B.1).

In this paper, we consider the following two minor adaptations of the generic MLCA mechanism described above:

1. **Balanced and global marginal economies:** In Lines 5–6 of Algorithm 2, MLCA draws for each bidder  $i \in N$  uniformly at random a set of marginal economies  $\tilde{N}$  to generate queries in this marginal economy. However, this implies that at the end of the auction it only holds on average that the same number of queries is asked from

**Algorithm 2:** MLCA( $Q^{\text{init}}, Q^{\max}, Q^{\text{round}}$ ) (Brero et al. 2021)

---

**Params:**  $Q^{\text{init}}, Q^{\max}, Q^{\text{round}}$  initial, max and #queries/round

```

1 foreach  $i \in N$  do
2   | Receive reports  $R_i$  for  $Q^{\text{init}}$  randomly drawn bundles
3 end
4 for  $k = 1, \dots, \lfloor (Q^{\max} - Q^{\text{init}}) / Q^{\text{round}} \rfloor$  do  $\triangleright$  Round iterator
5   | foreach  $i \in N$  do  $\triangleright$  Marginal economy queries
6     | Draw uniformly without replacement ( $Q^{\text{round}} - 1$ )
7       | bidders from  $N \setminus \{i\}$  and store them in  $\tilde{N}$ 
8       | foreach  $j \in \tilde{N}$  do
9         |  $q^{\text{new}} = q^{\text{new}} \cup \text{NextQueries}(N \setminus \{j\}, R_{-j})$ 
10        | end
11     |  $q^{\text{new}} = \text{NextQueries}(N, R)$   $\triangleright$  Main economy queries
12     | foreach  $i \in N$  do
13       | Receive reports  $R_i^{\text{new}}$  for  $q_i^{\text{new}}$ , set  $R_i = R_i \cup R_i^{\text{new}}$ 
14     | end
15 end
16 Given elicited reports  $R$  compute  $a_R^*$  as in Equation (1)
17 Given elicited reports  $R$  compute VCG-payments  $p(R)$ 
18 return Final allocation  $a_R^*$  and payments  $p(R)$ 

```

---

each bidder in each marginal economy. Moreover, since  $\tilde{N}$  is drawn fresh for each bidder this creates a computational overhead, since typically the WDPs in Line 8 in *NextQueries* needs to be solved more often. For example consider the case  $N = \{1, 2, 3, 4, 5, 6\}$ ,  $Q^{\text{round}} = 3$  and that for bidder 1 the  $Q^{\text{round}} - 1 = 2$  sampled marginal economies were given as  $\tilde{N} = \{3, 4\}$ , whilst for bidder 2,  $\tilde{N} = \{5, 6\}$ , and for bidder 3,  $\tilde{N} = \{1, 2\}$ . In this case, the WDPs in *NextQueries* would need to be already solved 6 times, which is the maximum possible. In our implementation, we change the following two things: First, we reduce the computational overhead by once globally selecting  $Q^{\text{round}}$  marginal economies in each iteration, i.e., we select a set  $\tilde{N}_{\text{global}}$  consisting of  $Q^{\text{round}}$  marginal economies before Line 5, and then select  $\tilde{N}$  for each bidder  $i \in N$  in the loop in Line 5 as admissible subset of size  $Q^{\text{round}} - 1$  of  $\tilde{N}_{\text{global}}$ . In the above example, if  $\tilde{N}_{\text{global}} = \{3, 4, 1\}$ , then this ensures that only  $Q^{\text{round}} = 3$  WDPs in the marginal economies are solved in one iteration. Second, we do not determine  $\tilde{N}_{\text{global}}$  uniformly at random, but ensure that at the end of the auction each marginal economy was selected equally often up to a difference in counts of at most one.

2. **Single training per iteration:** To further reduce computational overhead, we train each bidder's ML algorithm  $\mathcal{A}_i$  once at the beginning of each iteration, and then only select in *NextQueries* the trained  $\mathcal{A}_i$  corresponding to the active set of bidders  $I$ . This reduces the amount of total training procedures per iteration from (worst case)  $(1 + n) \cdot n$  to  $n$ .

### B Incentives of MLCA

In this section, we review the key arguments by Brero, Lubin, and Seuken (2021) why MLCA has good incentives in practice. First, we define VCG-payments given bidder's re-

ports.

**Definition B.1.** (VCG PAYMENTS FROM REPORTS) Let  $R = (R_1, \dots, R_n)$  denote an elicited set of reported bundle-value pairs from each bidder obtained from MLCA (Algorithm 2) and let  $R_{-i} := (R_1, \dots, R_{i-1}, R_{i+1}, \dots, R_n)$ . We then calculate the VCG payments  $p(R) = (p(R)_1, \dots, p(R)_n) \in \mathbb{R}_+^n$  as follows:

$$p(R)_i := \sum_{j \in N \setminus \{i\}} \hat{v}_j \left( (a_{R_{-i}}^*)_{j} \right) - \sum_{j \in N \setminus \{i\}} \hat{v}_j \left( (a_R^*)_{j} \right). \quad (16)$$

where  $a_{R_{-i}}^*$  maximizes the reported social welfare when excluding bidder  $i$ , i.e.,

$$a_{R_{-i}}^* \in \operatorname{argmax}_{a \in \mathcal{F}} \widehat{V}(a | R_{-i}) = \operatorname{argmax}_{a \in \mathcal{F}} \sum_{\substack{j \in N \setminus \{i\}; \\ (a_j, \hat{v}_j(a_j)) \in R_j}} \hat{v}_j(a_j), \quad (17)$$

and  $a_R^*$  is a reported-social-welfare-maximizing allocation (including all bidders), i.e.,

$$a_R^* \in \operatorname{argmax}_{a \in \mathcal{F}} \widehat{V}(a | R) = \operatorname{argmax}_{a \in \mathcal{F}} \sum_{i \in N: (a_i, \hat{v}_i(a_i)) \in R_i} \hat{v}_i(a_i). \quad (18)$$

Therefore, when using VCG, bidder  $i$ 's utility is:

$$u_i = v_i((a_R^*)_i) - p(R)_i \\ = v_i((a_R^*)_i) + \underbrace{\sum_{j \in N \setminus \{i\}} \hat{v}_j((a_R^*)_j)}_{\text{(a) Reported SW of main economy}} - \underbrace{\sum_{j \in N \setminus \{i\}} \hat{v}_j((a_{R_{-i}}^*)_j)}_{\text{(b) Reported SW of marginal economy}}.$$

Any beneficial misreport must increase the difference (a) – (b).

MLCA has two features that mitigate manipulations. First, MLCA explicitly queries each bidder's marginal economy (Algorithm 2, Line 5), which implies that (b) is practically independent of bidder  $i$ 's bid (Section 7.3 in (Brero, Lubin, and Seuken 2021) provides experimental support for this). Second, MLCA enables bidders to “push” information to the auction which they deem useful. This mitigates certain manipulations that target (a), as it allows bidders to increase (a) with truthful information. Brero, Lubin, and Seuken (2021) argue that any remaining manipulation would be implausible as it would require almost complete information.<sup>7</sup>

If we are willing to make two assumptions, we also obtain a theoretical incentive guarantee. Assumption 1 requires that, if all bidders bid truthfully, then MLCA finds an efficient allocation. Assumption 2 requires that, for all bidders  $i$ , if all other bidders report truthfully, then the social welfare of bidder  $i$ 's marginal economy is independent of his value reports. If both assumptions hold, then bidding truthfully is an ex-post Nash equilibrium in MLCA.

<sup>7</sup>In this paper, we propose a new method that uses a notion of epistemic uncertainty to actively explore regions of the bundle space with high uncertainty. Intuitively, this makes manipulation even harder, since additional exploration makes it more difficult for a bidder to prevent other bidders from getting queries in certain regions.

## C BO Perspective of ICAs

In this section, we discuss the Bayesian optimization (BO) perspective of iterative combinatorial assignment. Specifically, we analyze the MLCA mechanism (see Section 2.2 for an overview or Appendix A for a detailed description) in the light of BO.

### C.1 Bayesian Optimization Background

Bayesian optimization (BO) refers to class of *machine learning-based gradient-free* optimization methods, which for a given black-box objective function  $f : X \rightarrow Y$ , aims to solve

$$\max_{x \in X} f(x) \quad (19)$$

in an *iterative* manner (for costly function-evaluations). Specifically, given a budget of  $T$  queries (i.e., function evaluations of  $f$ ), a BO algorithm generates queries  $\{x^{(1)}, \dots, x^{(T)}\}$  with the aim that

$$f \left( \operatorname{argmax}_{x \in \{x^{(1)}, \dots, x^{(T)}\}} f(x) \right) \approx \max_{x \in X} f(x) \quad (20)$$

In each BO-step  $t$ , the algorithm selects an new input point  $x^{(t+1)} \in X$  and observes a (potentially noisy) output

$$y_t = f(x_t) + \varepsilon_t, \quad (21)$$

where  $\varepsilon_t$  is typically assumed to be i.i.d. Gaussian distributed, i.e.,  $\varepsilon_t \sim \mathcal{N}(0, \sigma^2)$  (recall, that in this paper, we assume that  $\sigma^2 = 0$ ). The BO algorithm's decision rule for selecting the next query  $x^{t+1}$  is based on

1. A *probabilistic model* representing an (approximate) posterior distribution over  $f$  (e.g. Gaussian processes, NOMU, ensembles methods, BNNs, ...).
2. An *acquisition function*  $\mathcal{A} : X \rightarrow Y$  that uses this probabilistic model to determine the next query  $x^{t+1} \in \operatorname{argmax}_{x \in X} \mathcal{A}(x)$  by properly trading off *exploration* and *exploitation*. Popular examples of acquisition functions include the
  - *Upper uncertainty bound* (aka *upper confidence bound (UCB)*) (Srinivas et al. 2012),
  - *Expected improvement* (Frazier 2018, Section 4.1), or
  - *Thompson sampling*.

### C.2 BO Perspective of MLCA

Iterative combinatorial assignment can be seen as a combinatorial BO task with an expensive-to-evaluate function:

- The objective (e.g., social welfare) in general lacks known structure and when evaluating it (e.g., value queries) one only observes the objective at a single input point and no derivatives such that gradient-based optimization cannot be used.
- Typically one can only query a very limited amount of information to find an approximately optimal allocation, For example, in a real-world spectrum auction, the auctioneer can only ask each bidder to answer on the order of 100 value queries for different bundles of items, even

though the space of possible bundles is exponential in the number of items  $m$ , i.e., there are  $2^m$  possible bundles and  $(n+1)^m$  possible allocations.

In this paper, we extend prior work on MLCA with a notion of uncertainty that makes MLCA more similar to classical BO. Specifically, we now use as acquisition function an upper uncertainty bound (uUB) represented as MVNN. This allows MLCA to trade-off exploration and exploitation making it more likely to find optimal allocations.

However, in addition to the challenges that arise in BO, combinatorial assignment adds their own set of challenges. For example, Gaussian Process-based BO often does not extend beyond 10-20 input dimension, which is problematic as in combinatorial assignment the input space can be much larger, e.g. for  $m = 98$  items and  $n = 10$  bidder the input space would be 980 dimensional (MRVM). In addition, integrality constraints to obtain only whole items (i.e., combinatorial assignment deals with assigning  $m$  *indivisible* items to agents, and thus one cannot assign for example  $1/2$  a item) and feasibility constraints that ensure to allocate each item only once to a single agent are often only incorporated via rounding or randomization.

Our work addresses both problems by combining (MV)NN-based MLCA by (Weissteiner and Seuken 2020; Weissteiner et al. 2022a) with the recently introduced NOMU Heiss et al. (2022), an optimization-based method to obtain uncertainty estimates for the prediction of NNs. Importantly, NOMU enables to represent a uUB as a *single* NN in contrast to other more expensive methods such as ensembles. Thus, NOMU is particularly suited for iterative combinatorial assignment, where uUB-based WDPs are solved hundreds of times to generate informative queries.

Recently, Papalexopoulos et al. (2022) also proposed a MILP-based BO method using ReLU NNs as surrogate model. They use ReLU NNs as surrogate model and Thompson sampling as acquisition function. Concretely, Papalexopoulos et al. (2022) approximate Thompson sampling via retraining a NN from scratch with a new random initialization. Subsequently, they determine the next query, by solving a NN-based MILP. However, unlike our proposal, Papalexopoulos et al. (2022) use no notion of uncertainty, making their approach fundamentally very similar to the (MV)NN-based MLCA by (Weissteiner and Seuken 2020; Weissteiner et al. 2022a).

## D NOMU for for Monotone NNs

In this section we give more details regarding our uncertainty estimates for monotonically increasing functions based on NOMU (see Section 3.1).

### D.1 Proof of Theorem 1

The 100% uUB  $f^{100\%-uUB}(x) := \sup_{f \in \mathcal{H}_{D^{\text{train}}}} f(x)$  is defined via a  $2^m$ -dimensional optimization problem with  $n^{\text{train}}$  constraints. In the following proof, we analytically derive the explicit closed-form joint solution of  $2^m$  such optimization problems (one for each  $x$ ), which we can represent as an MVNN that does not require any optimization algorithm.

*Proof of Theorem 1.* In the 1<sup>st</sup> part of the proof (which is based on the proof of Weissteiner et al. (2022a, Theorem 1)), we explicitly construct  $\mathcal{M}_i^{100\%-uUB}$  and show that  $\mathcal{M}_i^{100\%-uUB} \in \mathcal{V}_{D^{\text{train}}}$ . Equation (26) gives our explicit (fast to evaluate) closed-form formula for  $\mathcal{M}_i^{100\%-uUB}$ , which can be directly written down without any training-algorithm.

The 2<sup>nd</sup> part of the proof (which is new) shows that  $\mathcal{M}_i^{100\%-uUB}$  is actually the 100% uUB by showing that it is maximal (and thus the supremum is actually a maximum).

1. Let  $\hat{v}_i \in \mathcal{V}$  and let  $D^{\text{train}} = \{(x^{(l)}, \hat{v}_i(x^{(l)}))\}_{l=1}^{n^{\text{train}}}$  be a set of  $n^{\text{train}}$  observed training points corresponding to  $\hat{v}_i$ . First, given  $D^{\text{train}}$ , we construct an MVNN  $\mathcal{M}_i^{100\%-uUB}$  with weights  $\theta = (W_{D^{\text{train}}}^i, b_{D^{\text{train}}}^i)$  such that  $\mathcal{M}_i^{100\%-uUB}(x) = f^{100\%-uUB}(x)$  for all  $x \in \mathcal{X}$ .

Recall, that by definition  $\hat{v}_i((0, \dots, 0)) = 0$  and that we assume that  $((1, \dots, 1), \hat{v}_i((1, \dots, 1))) \in D^{\text{train}}$ . Now let  $(w_l)_{l=0}^{n^{\text{train}}}$  denote the observed/known values corresponding to  $\hat{v}_i$  sorted in increasing order, i.e. let  $x^{(0)} = (0, \dots, 0)$  with

$$w_0 := \hat{v}_i(x^{(0)}) = 0, \quad (22)$$

let  $x^{(n^{\text{train}})} = (1, \dots, 1)$  with

$$w_{n^{\text{train}}} := \hat{v}_i(x^{(n^{\text{train}})}), \quad (23)$$

and  $x^{(j)}, x^{(k)} \in \mathcal{X} \setminus \{x^{(0)}, x^{(n^{\text{train}})}\}$  for  $0 < j < k \leq n^{\text{train}} - 1$  with

$$w_j := \hat{v}_i(x^{(j)}) \leq w_k := \hat{v}_i(x^{(k)}). \quad (24)$$

In the following, we slightly abuse the notation and write for  $x^{(j)}, x^{(k)} \in \mathcal{X}$ ,  $x^{(j)} \subseteq x^{(k)}$  iff for the corresponding sets  $A^j, A^k \in 2^M$  it holds that  $A^j \subseteq A^k$ . Furthermore, we denote by  $\langle \cdot, \cdot \rangle$  the Euclidean scalar product on  $\mathbb{R}^m$ . Before we show that our construction fulfills  $\mathcal{M}_i^{100\%-uUB} \in \mathcal{V}_{D^{\text{train}}}$ , we define it as

$$\begin{aligned} \mathcal{M}_i^{100\%-uUB}(x) &:= \sum_{k=0}^{n^{\text{train}}-1} (w_{k+1} - w_k) \mathbb{1}_{\{\forall j \in \{0, \dots, k\} : x \not\subseteq x^{(j)}\}} \\ &= \sum_{k=0}^{n^{\text{train}}-1} (w_{k+1} - w_k) \varphi_{0,1} \left( \sum_{j=0}^k \varphi_{0,1} \left( \langle 1 - x^{(j)}, x \rangle \right) - k \right), \end{aligned} \quad (25)$$

where the second equality follows since

$$x \not\subseteq x^{(j)} \iff \langle 1 - x^{(j)}, x \rangle \geq 1 \quad (27)$$

$$\iff \varphi_{0,1} \left( \langle 1 - x^{(j)}, x \rangle \right) = 1, \quad (28)$$

which implies that

$$\forall j \in \{0, \dots, k\} : x \not\subseteq x^{(j)} \quad (29)$$

$$\iff \sum_{j=0}^k \varphi_{0,1} \left( \langle 1 - x^{(j)}, x \rangle \right) = k + 1, \quad (30)$$

and

$$\mathbb{1}_{\{\forall j \in \{0, \dots, k\} : x \not\subseteq x^{(j)}\}} = \varphi_{0,1} \left( \sum_{j=0}^k \varphi_{0,1} \left( \langle 1 - x^{(j)}, x \rangle \right) - k \right). \quad (31)$$

We now show that  $\mathcal{M}_i^{100\%-uUB}$  is actually a MVNN. Equation (26) can be equivalently written in matrix notation as

$$\underbrace{\begin{bmatrix} w_1 - w_0 \\ w_2 - w_1 \\ \vdots \\ w_{n^{\text{train}}} - w_{n^{\text{train}}-1} \end{bmatrix}}_{(W_{D^{\text{train}}}^{i,3})^\top \in \mathbb{R}_{\geq 0}^{n^{\text{train}}}} \varphi_{0,1} \left( W_{D^{\text{train}}}^{i,2} \varphi_{0,1} \left( \underbrace{\begin{bmatrix} 1 - x^{(1)} \\ 1 - x^{(2)} \\ \vdots \\ 1 - x^{(n^{\text{train}})} \end{bmatrix}}_{W_{D^{\text{train}}}^{i,1} \in \mathbb{R}_{\geq 0}^{(n^{\text{train}}) \times m}} x \right) + \underbrace{\begin{bmatrix} 0 \\ -1 \\ \vdots \\ -(n^{\text{train}} - 1) \end{bmatrix}}_{b_{D^{\text{train}}}^{i,2} \in \mathbb{R}_{\leq 0}^{n^{\text{train}}}} \right)$$

with  $W_{D^{\text{train}}}^{i,2} \in \mathbb{R}_{\geq 0}^{(n^{\text{train}}) \times (n^{\text{train}})}$  a lower triangular matrix of ones, i.e.,

$$W_{D^{\text{train}}}^{i,2} := \begin{bmatrix} 1 & 0 & \dots & 0 \\ \vdots & \ddots & \ddots & \vdots \\ \vdots & & \ddots & 0 \\ 1 & \dots & \dots & 1 \end{bmatrix}.$$

From that, we can see that  $\mathcal{M}_i^{100\%-uUB}$  is indeed a MVNN with four layers in total (i.e., two hidden layers) and respective dimensions  $[m, n^{\text{train}}, n^{\text{train}}, 1]$ . From Equation (25) we can see that for all  $l = 0, \dots, n^{\text{train}}$  :  $\mathcal{M}_i^{100\%-uUB}(x^{(l)}) = \hat{v}_i(x^{(l)})$  and therefore  $\mathcal{M}_i^{100\%-uUB} \in \mathcal{V}_{D^{\text{train}}}$ .

- Now we have to check what happens for  $x \in \mathcal{X} : (x, \hat{v}_i(x)) \notin D^{\text{train}}$ . Therefore, let  $x \in \mathcal{X} : (x, \hat{v}_i(x)) \notin D^{\text{train}}$ . Then, by definition we get that  $\mathcal{M}_i^{100\%-uUB}(x) = w_k$ , where  $k \in \{0, \dots, n^{\text{train}}\}$  is the smallest integer such that  $x \subseteq x^{(k)}$ . Assume there exists an  $h \in \mathcal{V}_{D^{\text{train}}}$  with  $h(x) > \mathcal{M}_i^{100\%-uUB}(x) = w_k = h(x^{(k)})$ . However, since  $x \subseteq x^{(k)}$  this is a contradiction to  $h$  fulfilling the monotonicity property. Thus, we get that  $\mathcal{M}_i^{100\%-uUB}(x) = \max_{f \in \mathcal{V}_{D^{\text{train}}}} f(x)$ . Since  $x$  was chosen arbitrarily we finally get that  $\mathcal{M}_i^{100\%-uUB}(x) = \max_{f \in \mathcal{V}_{D^{\text{train}}}} f(x)$  for all  $x \in \mathcal{X}$  which concludes the proof.  $\square$

## D.2 ICA-based New NOMU Architecture

In this section, we provide more details on our carefully chosen ICA-based new NOMU architecture. The original NOMU architecture from (Heiss et al. 2022) outputs a mean prediction  $\hat{f}$ , which is in our case the mean-MVNN  $\mathcal{M}_i^{\text{mean}}$  and an model uncertainty prediction  $\hat{\sigma}_f$ . Then, uUBs in the original NOMU algorithm at an input point  $x$  are defined as  $\hat{f}(x) + c \cdot \hat{\sigma}_f(x)$ .

### Monotone uUBs and Non-Monotone $\hat{\sigma}_f$

**Monotone Value Functions Imply Monotone uUBs.** Knowing that the unknown ground truth function is monotonically increasing<sup>8</sup> means that the support of the prior

<sup>8</sup>Within this paper “monotonically increasing” should always be interpreted as “monotonically non-decreasing”.

in function space only contains monotonically increasing functions in Bayesian language. In frequentist language this means that the hypothesis class  $\mathcal{H}$  only contains monotonically increasing functions. In both cases the resulting uUBs are monotonically increasing as well which we now mathematically prove in Propositions 1 and 2.

**Proposition 1.** Let  $\mathbb{P}[f \text{ is monotonically increasing}] = 1$  according to the prior and let  $uUB_\alpha(x) := \inf\{y \in \mathbb{R} : \mathbb{P}[f(x) \leq y | D^{\text{train}}] \geq \alpha\} \forall x \in X$  be the  $\alpha$ -credible upper bound (i.e., the  $\alpha$ -quantile of the posterior distribution of  $f(x)$ ).<sup>9</sup> Then it holds that  $uUB_\alpha(x)$  is monotonically increasing (i.e.,  $x \leq \tilde{x} \implies uUB_\alpha(x) \leq uUB_\alpha(\tilde{x})$ ).

*Proof.* Let  $x \leq \tilde{x}$ . For a shorter notation we write “ $f$  is (M)” instead of “ $f$  is monotonically increasing” and we define  $\tilde{\mathcal{V}} := \{f \in Y^X : f \text{ is (M)}\}$ . Then, from the definition of monotonicity, it follows for every  $y \in \mathbb{R}$  that<sup>10</sup>

$$\begin{aligned} \{f : f(x) > y, f \text{ is (M)}\} &\subseteq \{f : f(\tilde{x}) > y, f \text{ is (M)}\} \\ \iff \{f : f(x) > y\} \setminus \tilde{\mathcal{V}}^c &\subseteq \{f : f(\tilde{x}) > y\} \setminus \tilde{\mathcal{V}}^c \\ \iff \mathbb{P}[\{f : f(x) > y\} | D^{\text{train}}] &\leq \mathbb{P}[\{f : f(\tilde{x}) > y\} | D^{\text{train}}] \\ \iff \mathbb{P}[\{f : f(x) \leq y\} | D^{\text{train}}] &\geq \mathbb{P}[\{f : f(\tilde{x}) \leq y\} | D^{\text{train}}] \end{aligned}$$

Since  $uUB_\alpha(x)$  is the infimum, we know that for every  $y < uUB_\alpha(x)$ :

$$\mathbb{P}[\{f : f(\tilde{x}) \leq y\} | D^{\text{train}}] \leq \mathbb{P}[\{f : f(x) \leq y\} | D^{\text{train}}] < \alpha.$$

This means that every  $y < uUB_\alpha(x)$  is too small to be equal to  $uUB_\alpha(\tilde{x})$ , thus  $uUB_\alpha(x) \leq uUB_\alpha(\tilde{x})$ .  $\square$

**Proposition 2.** Let  $\mathcal{H}$  be a hypothesis class that only contains monotonically increasing functions and let  $uUB_{\mathcal{H}}(x) := \sup\{f(x) : f \in \mathcal{H}_D^{\text{train}}\}$  be an uUB, then  $uUB_{\mathcal{H}}$  is monotonically increasing (i.e.,  $x \leq \tilde{x} \implies uUB_{\mathcal{H}}(x) \leq uUB_{\mathcal{H}}(\tilde{x})$ ).

*Proof.* Let  $x \leq \tilde{x}$ , then  $\sup\{f(x) : f \in \mathcal{H}_D^{\text{train}}\} \leq \sup\{f(\tilde{x}) : f \in \mathcal{H}_D^{\text{train}}\}$ , since  $\forall f \in \mathcal{H}_D^{\text{train}} : f(x) \leq f(\tilde{x})$ .  $\square$

**Monotone Value Functions Do Not Imply Monotone Uncertainty.** However, the model uncertainty  $\hat{\sigma}_f$  (defining the width of the UBs) is *not* monotonic at all. For already observed training input points there is zero model uncertainty while smaller unobserved input points can have much bigger model uncertainty.

If one would simply use the prior knowledge about the monotonicity to improve the mean prediction (by assuring its monotonicity) but then estimate the uUB by simply adding a standard (e.g. original NOMU or GP) estimator for the (scaled) model uncertainty  $c \cdot \hat{\sigma}_f$  to the mean prediction

<sup>9</sup>In the literature,  $\mathbb{P}[f(x) \leq y | D^{\text{train}}, x]$  is often used instead of  $\mathbb{P}[f(x) \leq y | D^{\text{train}}]$  which is equal for every given  $x \in X$ . In both notations,  $f$  is seen as a random variable in function space.

<sup>10</sup>For the second equivalence we use that for every measurable set  $A$ , we obtain  $\mathbb{P}[A] - 0 = \mathbb{P}[A] - \mathbb{P}[\mathcal{V}^c] \leq \mathbb{P}[A \setminus \mathcal{V}^c] \leq \mathbb{P}[A]$ , thus  $\mathbb{P}[A \setminus \mathcal{V}^c] = \mathbb{P}[A]$ .

to obtain a uUB, one would obtain non-monotonic uUBs violating Propositions 1 and 2.

If one would simply use ensemble methods (Lakshminarayanan, Pritzel, and Blundell 2017; Gal and Ghahramani 2016) with MVNNs as ensemble members the uUBs obtained from the formula given in (Lakshminarayanan, Pritzel, and Blundell 2017; Gal and Ghahramani 2016) (re-stated in Heiss et al. (2022) for the noiseless case) would also lead to non-monotonic uUBs violating Propositions 1 and 2. In theory, this problem could be circumvented by directly using a certain quantile of the ensembles as uUB instead of calculating uUBs based on empirical mean and variance of the ensemble. However, even the 100%-quantile of the ensemble (the point-wise maximum of the ensemble predictions) would often not sufficiently capture enough uncertainty, since Heiss et al. (2022, Remark B.5) empirically showed that the uncertainty of ensemble methods often needs to be scaled up by a very big factor to capture enough uncertainty. Moreover, Kuleshov, Fenner, and Ermon (2018) empirically showed that the uncertainty (of ensemble methods) needs to be calibrated to achieve good results. To summarize, ensemble methods of monotonic functions have the problem that their calibration is limited or calibrating them results in non-monotonic uUBs. Note that the calibration method from Kuleshov, Fenner, and Ermon (2018) cannot solve this problem. Furthermore, in the ICA-setting of this paper the acquisition function optimization of the uUB obtained from deep ensembles (Lakshminarayanan, Pritzel, and Blundell 2017) would be computationally to expensive.

However, in the case of our proposed uUB  $\mathcal{M}_i^{\text{uUB}}$  the uncertainty can be calibrated by varying  $\pi_{\text{exp}}$  without scarifying monotonicity of the uUB. In the limit  $\pi_{\text{exp}} \rightarrow 0$  one would just obtain the mean prediction and in the limit  $\pi_{\text{exp}} \rightarrow \infty$  in relation to explicit and implicit regularization one would obtain the 100%-uUB as solution to our optimization problem.

**Linear Skip Connections** We have a hyper-parameter (that is part of our HPO) that decides whether we add a trainable linear connection directly from the input to the output for  $\mathcal{M}_i^{\text{uUB}}$  and  $\mathcal{M}_i^{\text{mean}}$  as formally defined in Definition F.1.

**No Connections Between the 2 Sub-architectures** The architecture suggested in Heiss et al. (2022) contains connections from the mean-sub-architecture to the uncertainty-sub-architecture (the dashed lines in (Heiss et al. 2022, Figure 2)). In our architecture (see Figure 1) we do not use such connections for two reasons:

1. Solving the WDP via the MILP given in Theorem 2 is computationally much faster because we can completely ignore  $\mathcal{M}_i^{\text{mean}}$  for the MILP formulation.
2. In the case of Heiss et al. (2022) the uncertainty would be completely disentangled from the mean prediction (or from the labels  $y^{\text{train}}$ ) without this connections prohibiting (Heiss et al. 2022, Desiderata D4). However, our architecture directly outputs the uUB instead of the uncertainty  $\sigma$ , thus  $\mathcal{M}_i^{\text{uUB}}$  is automatically not independent from the labels  $\hat{v}_i(x^{(l)})$

### D.3 ICA-based New NOMU Loss

**Definition D.1 (Smooth L1 Loss).** The smooth L1 loss  $L_1^\beta : \mathbb{R} \rightarrow \mathbb{R}$  with threshold parameter  $\beta \geq 0$  is defined as follows:

$$L_1^\beta(x, y) = \begin{cases} \frac{0.5}{\beta} \cdot (x - y)^2, & |x - y| \leq \beta \\ |x - y| - 0.5 \cdot \beta, & \text{otherwise.} \end{cases} \quad (32)$$

**Definition D.2 (Exponential Linear Unit (ELU)).** The ELU function  $ELU : \mathbb{R} \rightarrow \mathbb{R}$  (with default parameter  $\alpha = 1$ ) is defined as follows:

$$ELU(x) = \begin{cases} x, & x \geq 0 \\ 1 \cdot (\exp(x) - 1), & x < 0. \end{cases} \quad (33)$$

**Definition D.3 (Detailed ICA-based New NOMU Loss).** Let  $\pi = (\pi_{\text{sqr}}, \pi_{\text{exp}}, c_{\text{exp}}, \bar{\pi}, \underline{\pi}) \in \mathbb{R}_+^5$  be a tuple of hyperparameters. For a training set  $D^{\text{train}}$ ,  $L^\pi$  is defined as

$$L^\pi(\mathcal{M}_i^{\text{uUB}}) := \pi_{\text{sqr}} \sum_{l=1}^{n^{\text{train}}} L_1^\beta(\mathcal{M}_i^{\text{uUB}}(x^{(l)}), y^{(l)}) \quad (34a)$$

$$+ \pi_{\text{exp}} \int_{[0,1]^m} u(0.01 - c_{\text{exp}}(\min\{\mathcal{M}_i^{\text{uUB}}(x), \mathcal{M}_i^{100\%-\text{uUB}}(x)\} - \mathcal{M}_i^{\text{mean}}(x))) dx \quad (34b)$$

$$+ \pi_{\text{exp}} c_{\text{exp}} \bar{\pi} \int_{[0,1]^m} L_1^\beta((\mathcal{M}_i^{\text{uUB}}(x) - \mathcal{M}_i^{100\%-\text{uUB}}(x))^+) dx \quad (34c)$$

$$+ \pi_{\text{exp}} c_{\text{exp}} \underline{\pi} \int_{[0,1]^m} L_1^\beta((\mathcal{M}_i^{\text{mean}}(x) - \mathcal{M}_i^{\text{uUB}}(x))^+) dx \quad (34d)$$

$$+ \pi_{\text{sqr}} \sum_{l=1}^{n^{\text{train}}} 0.001(\mathcal{M}_i^{\text{uUB}}(x^{(l)} - y^{(l)})^+ + 0.5L_1^\beta((\mathcal{M}_i^{\text{uUB}}(x^{(l)} - y^{(l)})^+, 0)) \quad (34e)$$

where  $L_1^\beta$  is the smooth L1-loss with threshold  $\beta$  (see Definition D.1),  $(\cdot)^+$  the positive part, and  $u := 1 + ELU$  is convex monotonically increasing with ELU being exponential linear unit (ELU) (see Definition D.2).

Detailed interpretations of all five terms (including (34e) which was added to slightly improve the numerical stability) are as follows:

(34a) enforces that  $\mathcal{M}_i^{\text{uUB}}$  fits through the training data.

(34b) pushes  $\mathcal{M}_i^{\text{uUB}}$  up as long as it is below the 100%-uUB  $\mathcal{M}_i^{100\%-\text{uUB}}$ . This force gets weaker the further  $\mathcal{M}_i^{\text{uUB}}$  is above the mean  $\mathcal{M}_i^{\text{mean}}$  (especially if  $c_{\text{exp}}$  is large).  $\pi_{\text{exp}}$  controls the overall strength of (6b) and  $c_{\text{exp}}$  controls how fast this force increases when  $\mathcal{M}_i^{\text{uUB}} \rightarrow \mathcal{M}_i^{\text{mean}}$ . Thus, increasing  $\pi_{\text{exp}}$  increases the uUB and increasing  $c_{\text{exp}}$  increases the uUBs in regions where it is close to the mean. Weakening (6b) (i.e.,  $\pi_{\text{exp}} c_{\text{exp}} \rightarrow 0$ ) leads  $\mathcal{M}_i^{\text{uUB}} \approx \mathcal{M}_i^{\text{mean}}$ . Strengthening (6b) by increasing  $\pi_{\text{exp}} c_{\text{exp}}$  in relation to regularization<sup>11</sup> leads  $\mathcal{M}_i^{\text{uUB}} \approx \mathcal{M}_i^{100\%-\text{uUB}}$ . In practice, we obtain reasonable approximations to  $\alpha\%$ -uUB with  $\alpha \in [50, 100]$  depending on the value of  $\pi_{\text{exp}} c_{\text{exp}}$  in relation to regularization.

<sup>11</sup>Regularization can be early stopping or a small number of neurons (implicit) or L2-regularization on the parameters (explicit). The same principle would also hold true if one uses other forms of regularization such as L1-regularization or dropout.

(34c) enforces that  $\mathcal{M}_i^{\text{uUB}} \leq \mathcal{M}_i^{100\%-u\text{UB}}$ . In theory, (6c) would be redundant in the limit  $\pi_{\text{sqr}} \rightarrow \infty$ , because  $\mathcal{M}_i^{\text{uUB}} \in \mathcal{V}_{D^{\text{train}}}$ . The strength of this term is determined by  $\bar{\pi} \cdot (\pi_{\text{exp}} c_{\text{exp}})$ , where  $\bar{\pi}$  is the (6c)-specific hyperparameter and  $\pi_{\text{exp}} c_{\text{exp}}$  adjusts the strength of (6c) to (6b).

(34d) enforces  $\mathcal{M}_i^{\text{uUB}} \geq \mathcal{M}_i^{\text{mean}}$ . In theory, one should take the limit  $\bar{\pi} \rightarrow \infty$ . However, in practice, a moderate value of  $\bar{\pi}$  is numerically more stable and typically enforces that  $\mathcal{M}_i^{\text{uUB}} \geq \mathcal{M}_i^{\text{mean}}$ . The interpretation of  $\bar{\pi}$  and  $\pi_{\text{exp}} c_{\text{exp}}$  is analogous to (6c).

(34e) is an asymmetric version of (34a) for numerical stability. Since (34b) pushes  $\mathcal{M}_i^{\text{uUB}}$  for all  $x \in \mathcal{X}$  upwards,  $\mathcal{M}_i^{\text{uUB}}$  would have a tendency to give slightly too high predictions for training data points, but (34e) compensates this effect for slightly improved numerical stability. In theory (34e) would be redundant in the limit  $\pi_{\text{sqr}} \rightarrow \infty$ .

As in (Heiss et al. 2022), in the implementation of  $L^\pi$ , we approximate Equations (6b) to (6d) via MC-integration using additional, *artificial input points*  $D^{\text{art}} := \{x^{(l)}\}_{l=1}^{n^{\text{art}}}$  i.i.d.  $\text{Unif}([0, 1]^m)$ , where we sample new artificial input points for each batch of our mini-batch gradient descent based training algorithm.

Furthermore, note that in practice we train  $\mathcal{M}_i^{\text{mean}}$  and  $\mathcal{M}_i^{\text{uUB}}$  simultaneously but where  $\mathcal{M}_i^{\text{mean}}$  is *detached* in the loss  $L^\pi$  such that  $L^\pi$  does not influence the vanilla MVNN mean prediction  $\mathcal{M}_i^{\text{mean}}$ .

## E Parameter Initialization for MVNNs

In this section, we provide more details on our new parameter initialization method for MVNNs (see Section 3.2). Specifically, we give recommendations on how to set the hyperparameters of our proposed i.i.d. mixture distribution depending on the architecture size of the considered MVNN.

### E.1 Theoretical Results

**Definition E.1** (Mixture Distribution). *We define the probability density  $g_{A_k, B_k, p_k}$  of an initial weight  $W_{j,l}^{i,k}$  corresponding to an MVNN as<sup>12</sup>*

$$g_{A_k, B_k, p_k}(w) = \frac{1-p_k}{A_k} \mathbb{1}_{[0, A_k]}(w) + \frac{p_k}{B_k} \mathbb{1}_{[0, B_k]}(w), \quad (35)$$

which corresponds to a mixture distribution of  $\text{Unif}[0, A_k]$  and  $\text{Unif}[0, B_k]$ .

We assume that each  $W_{j,l}^{i,k}$  in the  $k$ -th layer is distributed according to Definition E.1. Then we obtain

$$\mu_k = \mathbb{E} \left[ W_{j,l}^{i,k} \right] = (1-p_k)A_k + p_k B_k. \quad (36)$$

<sup>12</sup>The bidder index  $i$  is not relevant in this section and we assume that each bidder  $i$  has the same architecture. If bidders would have different layer widths  $d^{i,k-1}$ , then all the values  $A_k, B_k, p_k, \mu_k, \sigma_k$  would depend on the bidder index  $i$  too, i.e.,  $A_{i,k}, B_{i,k}, p_{i,k}, \mu_{i,k}, \sigma_{i,k}$ .

Moreover, by using that the variance of an  $\text{Unif}[0, c]$ -distributed random variable is  $\frac{c^2}{12}$  we get that

$$\sigma_k^2 = \mathbb{V} \left[ W_{j,l}^{i,k} \right] = (1-p_k) \frac{A_k^2}{3} + p_k \frac{B_k^2}{3} - \mu_k^2. \quad (37)$$

In the following, we provide a rule how to set for each layer  $k$ ,  $A_k, B_k$  and  $p_k$  depending on the dimension  $d^{i,k-1}$  of the previous  $(k-1)$ st layer.

This rule ensures that the conditional expectation and the conditional variance are equal to two constants  $\mathbb{E}^{\text{init}}$ , and  $\mathbb{V}^{\text{init}}$ ,<sup>13</sup> which are independent of the dimension of the previous layer  $d^{i,k-1}$ . More formally, let  $z^{i,k-1} \in \mathbb{R}^{d^{i,k-1}}$  be the output of the neurons in the  $(k-1)$ st layer, then we set  $A_k, B_k$  and  $p_k$  such that

$$\mathbb{E} \left[ (W^{i,k} z^{i,k-1})_j + b_j^{i,k} \mid z^{i,k-1} = (1, \dots, 1)^\top \right] \stackrel{!}{=} \mathbb{E}^{\text{init}} \quad (38a)$$

$$\mathbb{V} \left[ (W^{i,k} z^{i,k-1})_j \mid z^{i,k-1} = (1, \dots, 1)^\top \right] \stackrel{!}{=} \mathbb{V}^{\text{init}}. \quad (38b)$$

**Remark E.1.** *Equivalent formulations of (38a) are*

$$(38a) \Leftrightarrow \mathbb{E} \left[ (W^{i,k} (1, \dots, 1)^\top)_j + b_j^{i,k} \right] \stackrel{!}{=} \mathbb{E}^{\text{init}} \\ \Leftrightarrow \mathbb{E} \left[ (W^{i,k} z^{i,k-1})_j + b_j^{i,k} \mid \overline{z^{i,k-1}} = 1 \right] \stackrel{!}{=} \mathbb{E}^{\text{init}},$$

where  $\overline{z^{i,k-1}} = \frac{1}{d^{i,k-1}} \sum_{l=1}^{d^{i,k-1}} z_l^{i,k-1}$ . And equivalent formulations of (38b) are

$$(38b) \Leftrightarrow \mathbb{V} \left[ (W^{i,k} (1, \dots, 1)^\top)_j \right] \stackrel{!}{=} \mathbb{V}^{\text{init}} \\ \Leftrightarrow \mathbb{V} \left[ (W^{i,k} z^{i,k-1})_j \mid z^{i,k-1} \right] \stackrel{!}{=} \mathbb{V}^{\text{init}} \overline{(z^{i,k-1})^2},$$

where  $\overline{(z^{i,k-1})^2} = \frac{1}{d^{i,k-1}} \sum_{l=1}^{d^{i,k-1}} (z_l^{i,k-1})^2$ .

The solution to problem (38) is not unique, but we propose three hyperparameters  $B^{\text{init}}, b^{\text{init}}, \epsilon \in \mathbb{R}_+$  to characterize one specific solution that has multiple nice properties (see Theorem 3).

**Definition E.2** (Scaling Rule). *For any choice of hyperparameters  $\mathbb{E}^{\text{init}}, \mathbb{V}^{\text{init}}, B^{\text{init}}, b^{\text{init}}, \epsilon \in \mathbb{R}_+$  we propose the following values for  $B_k, A_k$  and  $p_k$  (for a shorter notation we*

<sup>13</sup>Note that  $\text{init}_E = \mathbb{E}^{\text{init}} = (38a)$  includes already the bias, while  $\text{init}_V = \mathbb{V}^{\text{init}}$  does not include the bias. But this is a simple additive term that could easily be adjusted. One could easily include the bias in both or in none of them to make it more consistent.

write  $d$  instead of  $d^{i,k-1} \in \mathbb{N}_+$ :

$$B_k = \begin{cases} \max\left(\frac{3\mathcal{M}_k^2 + 3d\mathbb{V}^{init}}{2\mathcal{M}_k d} + \frac{\epsilon}{d}, B^{init}\right) & , d > \frac{\mathcal{M}_k^2}{3\mathbb{V}^{init}} \\ \frac{2}{d^{i,k}} \mathcal{M}_k & , \text{else} \end{cases} \quad (39)$$

$$p_k = \begin{cases} 1 - \frac{B_k^2 d^2 - 4B_k \mathcal{M}_k d + 4\mathcal{M}_k^2}{B_k^2 d^2 - 4B_k \mathcal{M}_k d + 3\mathcal{M}_k^2 + 3d\mathbb{V}^{init}} & , d > \frac{\mathcal{M}_k^2}{3\mathbb{V}^{init}} \\ 1 & , \text{else} \end{cases} \quad (40)$$

$$A_k = \begin{cases} \frac{2\mathcal{M}_k - B_k d p_k}{d(1-p_k)} & , d > \frac{\mathcal{M}_k^2}{3\mathbb{V}^{init}} \\ 0 & , \text{else,} \end{cases} \quad (41)$$

$$W_{j,l}^{i,k} \stackrel{i.i.d.}{\sim} g_{A_k, B_k, p_k} \quad (42)$$

$$b_j^{i,k} \stackrel{i.i.d.}{\sim} \text{Unif}[-b^{init}, 0] \quad (43)$$

where  $\mathcal{M}_k = \mathbb{E}^{init} + \frac{b^{init}}{2}$  and where  $g_{A_k, B_k, p_k}$  is the mixture distribution described in Definition E.1 and where all weights and biases are sampled independently.

Finally, when using the scaling rule from Definition E.2, we can prove the following theorem.

**Theorem 3.** For any choice of hyperparameters  $\mathbb{E}^{init}, \mathbb{V}^{init}, B^{init}, b^{init}, \epsilon \in \mathbb{R}_+$ , for every  $k \in \{1, \dots, K_i\}$ , for every dimension  $d^{i,k-1} \in \mathbb{N}_+$  it holds that if we sample according to the distribution described in Definition E.2, we obtain that:<sup>14</sup>

1. (38a) holds,
2.  $\mathbb{V}\left[(W^{i,k} z^{i,k-1})_j \mid z^{i,k-1} = (1, \dots, 1)^\top\right] \geq \mathbb{V}^{init}$  holds,
3. (38b) holds if  $d^{i,k-1} > \frac{\mathcal{M}_k^2}{3\mathbb{V}^{init}}$ ,
4.  $\mathbb{P}\left[W_{j,l}^{i,k} = 0\right] = 0$  if  $\epsilon > 0$
5.  $\mathbb{P}\left[W_{j,l}^{i,k} = 0\right] = 1 - p_k$  if  $\epsilon = 0$  and  $B^{init} \leq B_k$ ,
6.  $\mathbb{P}\left[W_{j,l}^{i,k} < 0\right] = 0$ ,
7.  $\mathbb{P}\left[W_{j,l}^{i,k} > B_k\right] = 0$ ,
8.  $B_k \geq \frac{3\mathbb{V}^{init}}{2\mathcal{M}_k}$ ,
9.  $\lim_{d^{i,k-1} \rightarrow \infty} B_k = \max\left\{\frac{3\mathbb{V}^{init}}{2\mathcal{M}_k}, B^{init}\right\}$ .

*Proof.* First, note that<sup>15</sup>

$$\begin{aligned} (38a) &\Leftrightarrow \mathbb{E}\left[(W^{i,k} z^{i,k-1})_j + b_j^{i,k} \mid \overline{z^{i,k-1}} = 1\right] \stackrel{!}{=} \mathbb{E}^{init} \\ &\Leftrightarrow \mathbb{E}\left[(W^{i,k} z^{i,k-1})_j \mid \overline{z^{i,k-1}} = 1\right] \stackrel{!}{=} \mathbb{E}^{init} - \mathbb{E}\left[b_j^{i,k}\right] \\ &\Leftrightarrow d^{i,k-1} \mathbb{E}\left[W_{j,l}^{i,k}\right] \stackrel{!}{=} \mathbb{E}^{init} + \frac{b^{init}}{2} \\ &\Leftrightarrow \mathbb{E}\left[W_{j,l}^{i,k}\right] \stackrel{!}{=} \frac{\mathcal{M}_k}{d^{i,k-1}}. \end{aligned}$$

<sup>14</sup>We assume that  $\mathbb{E}^{init}, \mathbb{V}^{init}$  and  $d$  are strictly positive. However,  $B^{init}, b^{init}$  and  $\epsilon$  could in theory also be set to 0 and Theorem 3 is formulated such that it would still hold true for  $B^{init}, b^{init}, \epsilon \in \mathbb{R}_+ \cup \{0\}$ .

<sup>15</sup>For this calculation we use the seemingly more general formulation from Remark E.1, so that one can also see the proof of the part regarding (38a) in Remark E.1.

We prove this in section ‘‘Proof of item 1’’ of the **MATHEMATICA SCRIPT**<sup>16</sup>, where we use the notation  $d := d^{i,k-1}$ ,  $\mathbb{M} := \mathcal{M}_k$ ,  $\mathbb{V} := \mathbb{V}^{init}$ ,  $\epsilon := \epsilon$ ,  $B^{init} := B^{init}$ ,  $B^{choice} := B_k$  given in (39),  $p^{choice} := p_k$  given in (40),  $A^{choice} := A_k$  given in (41) and  $\mathbb{E}^{ofW} := \mathbb{E}\left[W_{j,l}^{i,k}\right]$  computed in (36). This proves item 1.

We manipulate

$$\begin{aligned} (38b) &\Leftrightarrow \mathbb{V}\left[(W^{i,k} z^{i,k-1})_j \mid z^{i,k-1} = (1, \dots, 1)^\top\right] \stackrel{!}{=} \mathbb{V}^{init} \\ &\Leftrightarrow d^{i,k-1} \mathbb{V}\left[W_{j,l}^{i,k}\right] \stackrel{!}{=} \mathbb{V}^{init} \\ &\Leftrightarrow \mathbb{V}\left[W_{j,l}^{i,k}\right] \stackrel{!}{=} \frac{\mathbb{V}^{init}}{d^{i,k-1}}. \end{aligned}$$

We prove this in section ‘‘Proof of item 2 and 3’’ of the **MATHEMATICA SCRIPT** with the additional notation  $\mathbb{V}^{ofW} := \mathbb{V}\left[W_{j,l}^{i,k}\right]$  computed in (37). This section proves items 2 and 3.

To show item 4 it is sufficient to show  $A_k > 0$  or  $p_k = 0$  and  $B_k > 0$  (because of  $A_k \leq B_k$ , as shown in section ‘‘Proof of item 7: (A ≤ B)’’). If  $d^{i,k-1} > \frac{\mathcal{M}_k^2}{3\mathbb{V}^{init}}$ , we show  $A_k > 0$  in section ‘‘Proof of item 4’’ of the **MATHEMATICA SCRIPT**. In the other case  $p_k = 0$  and  $B_k > 0$  as one can directly see from (40) and (39).

To show item 5, it is sufficient to show that  $A_k = 0$ , which we show in section ‘‘Proof of item 5’’ of the **MATHEMATICA SCRIPT** in the case  $d^{i,k-1} > \frac{\mathcal{M}_k^2}{3\mathbb{V}^{init}}$  and follows directly from (41) in the other case.

Item 6 follows directly from Definition E.1 and the fact that  $A_k \geq 0$  and  $B_k \geq 0$  (see section ‘‘Proof of item 6’’ in the **MATHEMATICA SCRIPT**).

Item 7 follows directly from Definition E.1 and  $A_k \leq B_k$  (see section ‘‘Proof of item 7: (A ≤ B)’’ in the **MATHEMATICA SCRIPT**).

Item 8 is shown for the two cases in section ‘‘Proof of item 8’’ of the **MATHEMATICA SCRIPT**.

Item 9 is shown in section ‘‘Proof of item 9’’ in our **MATHEMATICA SCRIPT**.  $\square$

**Discussion of Theorem 3.** Items 1 and 3 in Theorem 3 tell us that our initialization scheme actually solves problem (38) if  $d^{i,k-1} > \frac{\mathcal{M}_k^2}{3\mathbb{V}^{init}}$ . Note that problem (38) does not have any solution for for  $d^{i,k-1} \leq \frac{\mathcal{M}_k^2}{3\mathbb{V}^{init}}$  (as can be seen in

<sup>16</sup>You can open the **MATHEMATICA SCRIPT** including the results in your web-browser ([https://www.wolframcloud.com/obj/jakob.heiss/Published/MVNN\\_initialization.V1.nb](https://www.wolframcloud.com/obj/jakob.heiss/Published/MVNN_initialization.V1.nb)) without the need to install anything on your computer. (The interactive plot might only work if you open the script with an installed version of Mathematica, but it is not necessary for the proof.) We use a computer algebra system to make it much more convenient to check the correctness of our proof. Some of the terms that appear in this proof are already very long as one can see for example in section ‘‘Proof of item 2 and 3’’ in our **MATHEMATICA SCRIPT**. Simplifying these terms by hand would take multiple pages of very tedious calculations, which would be highly prone to typos and other mistakes. Within our **MATHEMATICA SCRIPT** we only use exact symbolic methods and no numerical approximations (except for the visualizations).



the first 5 line of our **MATHEMATICA SCRIPT** with the notation explained in the proof of Theorem 3). However, items 1 and 2 in Theorem 3 tell us that we still have a reasonable initialization scheme for  $d^{i,k-1} \leq \frac{\mathcal{M}_k^2}{3\mathbb{V}^{\text{init}}}$  that solves the relaxed problem of items 1 and 2. In practice solutions to this relaxed problem are still fine, since it also prevents us from exploding expectation or vanishing variance. Too much variance in the initialization is less of a problem.<sup>17</sup>

Items 4 and 5 motivate to choose  $\epsilon > 0$  to prevent weights being initialized to zero, which can lead to bad local minima.

Item 6 guarantees that our network is actually a valid MVNN at initialization fulfilling the non-negativity constraints of the weights at initialization.<sup>18</sup>

Items 7 to 9 give us guarantees on the upper bound of the weights.

## E.2 Recommended Hyperparameter Choices

In this section, we provide intuition about each hyperparameter  $\mathbb{E}^{\text{init}}, \mathbb{V}^{\text{init}}, B^{\text{init}}, b^{\text{init}}, \epsilon \in \mathbb{R}_+$  and recommendations on how to set them in practice.

1. **Parameter  $\mathbb{E}^{\text{init}}$ :** (`init_E` in our code) gives the conditional expectation (38a) of a pre-activated neuron (including bias) conditioned on  $z^{i,k-1} = 1$  (see item 1 in Theorem 3 and Remark E.1). This corresponds to an upper bound of the expected value of the MVNN  $\mathbb{E}[\mathcal{M}_i^\theta((1, \dots, 1))]$  (i.e., the predicted value of the full bundle) at initialization of the network, if all cutoffs  $t^{i,k}$  of the bReLU activation function are equal to 1.  $\mathbb{E}^{\text{init}}$  is approximately equal to  $\mathbb{E}[\mathcal{M}_i^\theta((1, \dots, 1))]$  if  $\mathbb{E}^{\text{init}} \geq 1$ .

If you normalize the data such that the full bundle has always value 1 (i.e.,  $\hat{v}_i((1, \dots, 1)) = 1$ ), setting  $\mathbb{E}^{\text{init}} = 1$  is our recommended choice. If you choose to initialize the bReLU cutoffs  $t^{i,k}$  i.i.d. uniformly at random, i.e.  $t^{i,k} \sim \text{Unif}(0, 1)$ , then  $\mathbb{E}^{\text{init}} \in [1, 2]$  is recommended, because then the right-hand side of the inequality<sup>19</sup>  $\mathbb{E}[o_j^{i,k}] = (\mathbb{E}^{\text{init}} - \mathbb{E}[b_j^{i,k}])\mathbb{E}[z^{i,k-1}] + \mathbb{E}[b_j^{i,k}] \leq (\mathbb{E}^{\text{init}} - \mathbb{E}[b_j^{i,k}])\mathbb{E}[t^{i,k-1}] + \mathbb{E}[b_j^{i,k}] = \frac{\mathbb{E}^{\text{init}} + b_j^{\text{init}}}{2} - \frac{b_j^{\text{init}}}{2} = \frac{\mathbb{E}^{\text{init}}}{2} - \frac{b_j^{\text{init}}}{4} \approx \frac{\mathbb{E}^{\text{init}}}{2}$  is an upper bound for  $\mathbb{E}[\mathcal{M}_i^\theta((1, \dots, 1))]$

<sup>17</sup>Alternatively one could consider to relax problem (38) in the other direction by allowing smaller expectation instead of bigger variance, which would also be fine in practice. A solution to this alternative relaxed problem could be simply achieved by changing the definition of  $B_k$  in the “else”-case of (39).

<sup>18</sup>Note that if we would initialize our network with a weight-distribution that solves problem (38), but does not fulfill Item 6 (e.g. a generic initialization with  $\mu_k = 0$  and  $\sigma_k \propto \frac{1}{\sqrt{d^{i,k-1}}}$ ), we would get a valid MVNN after the first gradient step, which projects all the negative weights to zero. However, this almost initial network would have exploding conditional expectations, i.e., almost all neurons would have pre-activations  $o_j^{i,k} > 1$  independent of the input training data point and thus one would end up with an almost constant function and zero gradients as shown in Figure 5.

<sup>19</sup>Recall, that  $o_j^{i,k}$  is the pre-activated value of the  $j$ -th neurons in the  $k$ -th layer (of the  $i$ -th bidder) including biases. E.g.,  $o_1^{i,K_i} = \mathcal{M}_i^\theta(x)$ .

at initialization.<sup>20</sup> If the values of your MVNN are in a different order of magnitude, you should scale your data in a pre-processing step to  $[0, 1]$ .

2. **Parameter  $\mathbb{V}^{\text{init}}$ :** (`init_V` in our code) gives the conditional variance (38b) of a pre-activated neuron (without bias) conditional on  $z^{i,k-1} = (1, \dots, 1)^\top$ , if  $d^{i,k-1} > \frac{\mathcal{M}_k^2}{3\mathbb{V}^{\text{init}}}$  (see item 3 in Theorem 3). In any case,  $\mathbb{V}^{\text{init}}$  is a lower bound for this conditional variance (see item 2 in Theorem 3). Typically, we select  $\mathbb{V}^{\text{init}} \in [1/50, 1]$ . Choosing  $\mathbb{V}^{\text{init}}$  too small yields an almost deterministic network initialization. Since we prefer initial weights that are smaller than one,  $\mathbb{V}^{\text{init}}$  should not be chosen too large (i.e., preferably  $\frac{3\mathbb{V}^{\text{init}}}{2\mathcal{M}_k} \leq 1$  because of items 7 to 9 in Theorem 3). If  $\mathbb{E}^{\text{init}}$  is in a different order of magnitude,  $\mathbb{V}^{\text{init}}$  should scale approximately with  $\sqrt{\mathbb{E}^{\text{init}}}$  or  $\mathbb{E}^{\text{init}}$ .
3. **Parameter  $b^{\text{init}}$ :** (`init_bias` in our code<sup>21</sup>) All the biases of the MVNN  $b_j^{i,k}$  are sampled uniformly at random from  $[-b^{\text{init}}, 0]$  as given in eq. (43). Setting  $b^{\text{init}} = 0.05$  is our recommendation, although any other small values would be sufficient. We discourage zero to avoid numerical issues during training.
4. **Parameter  $B^{\text{init}}$ :** (`init_b` in our code<sup>21</sup>) is a very technical parameter that is not really important as long as it is not too big. The “big” weights are sampled from  $\text{Unif}(0, B_k)$ , i.e.,  $B_k$  is an upper bound for the weights (see item 7 in Theorem 3). Usually, we prefer  $B_k$  that are not unnecessary big, but too small  $B_k$  leads to almost vanishing  $A_k$  (by a similar argument as item 5 in Theorem 3). This is why we want  $B_k$  to be not unnecessarily small.  $B^{\text{init}}$  gives a lower bound for  $B_k$  in the case of large number of neurons (see item 9 in Theorem 3 and (39)). Setting  $B^{\text{init}} = 0.05$  is our recommendation (but one could also use any other small value including zero).
5. **Parameter  $\epsilon$ :** (`init_little_const` in our code) prevents weights from being initialized to zero (i.e.,  $\epsilon > 0$  guarantees that no initial weight will be *exactly* zero, see item 4 in Theorem 3). Conversely setting  $\epsilon = 0$  leads weights to be zero with probability  $(1 - p_k)$  (see item 5 in Theorem 3). If one chooses  $\epsilon$  too large  $B_k$  can become too large (see (39)). Thus, setting  $\epsilon = 0.1$  is our recommendation (similarly to  $b^{\text{init}}$  any other small value is also admissible).

In the last section of our **MATHEMATICA SCRIPT** we provide an interactive plot that shows how  $B_k, A_k, p_k, \mathbb{V}[o_j^{i,k} - b_j^{i,k} | z^{i,k-1} = (1, \dots, 1)^\top]$  and  $\mathbb{E}[o_j^{i,k} | z^{i,k-1} = (1, \dots, 1)^\top]$  depend on  $d^{i,k-1}$  for

<sup>20</sup>On the other hand one could argue that one wants the conditional expectation of pre-activated neurons to be smaller because of the smaller cut-offs. However, note especially for small values of  $\mathbb{E}^{\text{init}}$ , the actual expectation  $\mathbb{E}[\mathcal{M}_i^\theta((1, \dots, 1))]$  at initialization decreases with increasing depth of the network, since the upper bound can loose its tightness as depth increases especially for  $\mathbb{E}^{\text{init}} < 1$ .

<sup>21</sup>Be careful, when translating the notation of our paper into the notation of our code.  $B_k$  is `b` in our code and the biases  $b$  are denoted by `bias` in our code.  $b^{\text{init}}$  does *not* translate to `init_b`.

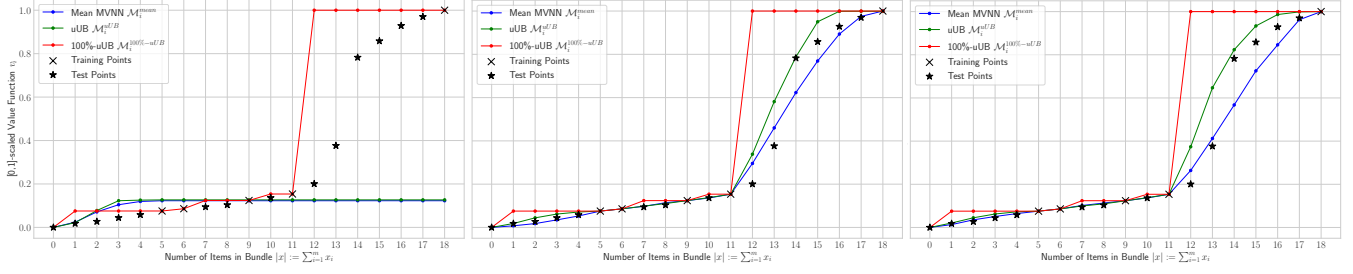


Figure 5:  $\mathcal{M}_i^{\text{mean}}$ ,  $\mathcal{M}_i^{\text{uUB}}$  and  $\mathcal{M}_i^{100\text{-uUB}}$  along an increasing 1D subset-path in LSVM for the national bidder. **Left:** [64,64]-architecture with generic initialization fails. **Middle:** [64,64]-architecture with our initialization works. **Right:** even larger [256,256]-architecture with our initialization still works.

different choices of our hyperparameters.

### E.3 Visualization for Wider MVNNs

Figure 5 confirms that our initialization method also properly works for an even larger MVNN-architecture with two hidden layers with 256 neurons per hidden layer. While the problems of the generic initialization methods described in Section 3.2 increase as the number of neurons increase, our initialization method can also deal with arbitrarily large number of neurons.

## F MLP

In this section we provide more details on Section 3.3.

### F.1 Proof of Theorem 2

In this section, we provide the proof of Theorem 2.

First, we show in Lemma 1 how to encode an arbitrary single hidden MVNN layer into multiple linear constraints. For this fix a bidder  $i \in N$  and an arbitrary layer  $k \in \{1, \dots, K_i - 1\}$ . Recall, that  $z^{i,k-1} \in \mathbb{R}^{d^{i,k-1}}$  denotes the output of the previous layer (with  $z^{i,0}$  being equal to the input  $x \in \mathbb{R}^{d^{i,0}} = \mathbb{R}^m$ ) and that  $o^{i,k} := W^{i,k} z^{i,k-1} + b^{i,k}$  denotes the *pre*-activated output of the  $k^{\text{th}}$  layer with  $l^{i,k} \leq o^{i,k} \leq u^{i,k}$ , where the tight lower/upper bound  $l^{i,k}/u^{i,k}$  can be computed by forward-propagating the empty/full package. Then the following Lemma holds:<sup>22</sup>

**Lemma 1.** Consider the following set of linear constraints:

$$z^{i,k} \leq \alpha^{i,k} \cdot t^{i,k} \quad (44)$$

$$z^{i,k} \leq o^{i,k} - l^{i,k} \cdot (1 - \alpha^{i,k}) \quad (45)$$

$$z^{i,k} \geq \beta^{i,k} \cdot t^{i,k} \quad (46)$$

$$z^{i,k} \geq o^{i,k} + (t^{i,k} - u^{i,k}) \cdot \beta^{i,k} \quad (47)$$

$$\alpha^{i,k} \in \{0, 1\}^{d^{i,k}}, \beta^{i,k} \in \{0, 1\}^{d^{i,k}}. \quad (48)$$

Then it holds for the output of the  $k^{\text{th}}$  layer  $\varphi_{0,t^{i,k}}(o^{i,k}) = z^{i,k}$ .

*Proof.* Recall, that  $o^{i,k} := W^{i,k} z^{i,k-1} + b^{i,k}$  denotes the preactivated output of the  $k^{\text{th}}$  layer. Let  $j \in \{1, \dots, d^{i,k}\}$

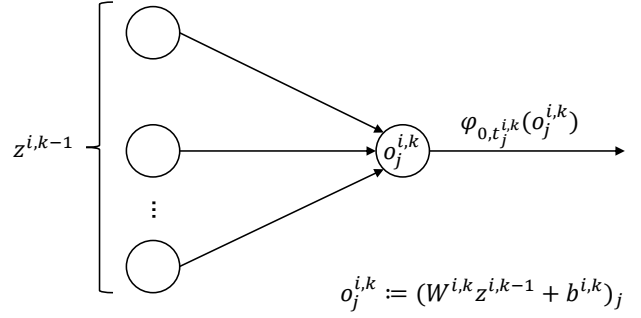


Figure 6: Schematic representation of the  $j^{\text{th}}$  neuron in the  $k^{\text{th}}$  layer. Shown are the output  $z^{i,k-1}$  of the previous  $(k-1)^{\text{st}}$  layer, the preactivated output  $o_j^{i,k}$  of the  $j^{\text{th}}$  neuron in the  $k^{\text{th}}$  layer, and the output of the  $j^{\text{th}}$  neuron of the  $k^{\text{th}}$  layer after applying bRELU  $\varphi_{0,t_j^{i,k}}(o_j^{i,k}) = \min(t_j^{i,k}, \max(0, o_j^{i,k}))$ .

denote the  $j^{\text{th}}$  neuron of that layer and let  $l_j^{i,k} \leq o_j^{i,k} \leq u_j^{i,k}$ , where  $l_j^{i,k}$  and  $u_j^{i,k}$  are the tight box bounds computed by forward propagating the empty, i.e.,  $x = (0, \dots, 0)$ , and the full, i.e.,  $x = (1, \dots, 1)$  bundle (see (Weissteiner et al. 2022a, Appendix C.5 and Fact C.1)). Moreover, let  $\varphi_{0,t_j^{i,k}}(o_j^{i,k}) = \min(t_j^{i,k}, \max(0, o_j^{i,k}))$  with  $t_j^{i,k} \geq 0$  be the output of the  $j^{\text{th}}$  neuron in the  $k^{\text{th}}$  layer. In Figure 6, we present a schematic representation for a single neuron. In Figure 7, we present an example of the bReLU activation function.

We distinguish the following three exclusive cases:

- **Case 1:**  $o_j^{i,k} < 0$ , i.e., the red line segment in Figure 7. Per definition it follows that  $\varphi_{0,t_j^{i,k}}(o_j^{i,k}) = 0$ . Setting  $\alpha_j^{i,k} = \beta_j^{i,k} = 0$  in Equations (44) to (48) implies that  $z_j^{i,k} = 0$ .
- **Case 2:**  $o_j^{i,k} \in [0, t_j^{i,k}]$ , i.e., the blue line segment in Figure 7. Per definition it follows that  $\varphi_{0,t_j^{i,k}}(o_j^{i,k}) = o_j^{i,k}$ . Setting  $\alpha_j^{i,k} = 1$  and  $\beta_j^{i,k} = 0$  in Equations (44) to (48) implies that  $z_j^{i,k} = o_j^{i,k}$ .

<sup>22</sup>All vector inequalities should be understood component-wise.

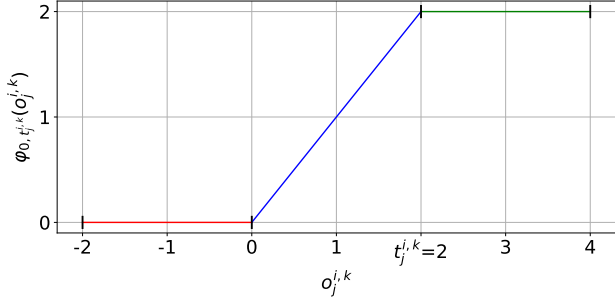


Figure 7: Example plot for agent  $i$ , layer  $k$  and neuron  $j$  of the bReLU activation function  $\varphi_{0,t_j^{i,k}}(\cdot) := \min(t_j^{i,k}, \max(0, \cdot))$  (Weissteiner et al. 2022a) with cutoff  $t_j^{i,k} = 2$  in the interval  $[-2, 4]$ . Shown are the preactivated output  $o_j^{i,k}$  of the  $j^{\text{th}}$  neuron in the  $k^{\text{th}}$  layer (x-axis) and the output of the  $j^{\text{th}}$  neuron in the  $k^{\text{th}}$  layer after applying bReLU (y-axis).

- **Case 3:**  $o_j^{i,k} > t_j^{i,k}$ , i.e., the green line segment in Figure 7. Per definition it follows that  $\varphi_{0,t_j^{i,k}}(o_j^{i,k}) = t_j^{i,k}$ . Setting  $\alpha_j^{i,k} = \beta_j^{i,k} = 1$  in Equations (44) to (48) implies that  $z_j^{i,k} = t_j^{i,k}$ .

Thus, in total  $z^{i,k} = \varphi_{0,t_j^{i,k}}(o_j^{i,k})$ .  $\square$

Using Lemma 1, we can now proof Theorem 2 which provides our new and more succinct MILP formulation.

*Proof.* Consider the ML-based WDP from Equation (7). For each bidder  $i \in N$ , we first set  $z^{i,0}$  equal to the input bundle  $a_i$ . Then we proceed by using Lemma 1 for  $k = 1$ , i.e., we reformulate the output of the 1<sup>st</sup> layer as the linear constraints Equations (44) to (47). We iterate this procedure until we have reformulated the last hidden layer, i.e, layer  $k = K_i - 1$ . Doing so for each bidder  $i \in N$  yields the desired MILP formulation from Theorem 2.  $\square$

## F.2 Removing Constraints via Box Bounds

Let  $l_j^{i,k} \leq o_j^{i,k} \leq u_j^{i,k}$ , where  $l_j^{i,k}$  and  $u_j^{i,k}$  are the *tight* box bounds computed by forward propagating the empty, i.e.,  $x = (0, \dots, 0)$ , and the full, i.e.,  $x = (1, \dots, 1)$  bundle (see (Weissteiner et al. 2022a, Appendix C.5 and Fact C.1)).

In the following cases, one can remove the constraints and corresponding variables in Lemma 1 and thus also in Theorem 2.

- **Case 1:**  $0 \leq t_j^{i,k} < l_j^{i,k} \leq u_j^{i,k}$ . Then one can simply set

$$z_j^{i,k} := t_j^{i,k} \quad (49)$$

and remove the  $j^{\text{th}}$  components from all constraints Equations (44) to (48) of the corresponding layer  $k$  ( $o_j^{i,k}$  lies for sure in the green line segment in Figure 7).

- **Case 2:**  $l_j^{i,k} \leq u_j^{i,k} < 0 \leq t_j^{i,k}$ . Then one can simply set

$$z_j^{i,k} := 0 \quad (50)$$

and remove the  $j^{\text{th}}$  components from all constraints Equations (44) to (48) of the corresponding layer  $k$  ( $o_j^{i,k}$  lies for sure in the red line segment in Figure 7).

- **Case 3:**  $0 \leq l_j^{i,k} \leq u_j^{i,k} \leq t_j^{i,k}$ . Then one can simply set

$$z_j^{i,k} := o_j^{i,k} \quad (51)$$

and remove the  $j^{\text{th}}$  components from all constraints Equations (44) to (48) of the corresponding layer  $k$  ( $o_j^{i,k}$  lies for sure in the blue line segment in Figure 7).

- **Case 4:**  $0 \leq l_j^{i,k} \leq t_j^{i,k} < u_j^{i,k}$ . Then one can set

$$\alpha_j^{i,k} := 1 \quad (52)$$

and only one binary decision variable for the  $j^{\text{th}}$  neuron of the  $k^{\text{th}}$  layer remains. ( $o_j^{i,k}$  lies for sure in the union of the blue and green line segment in Figure 7).

- **Case 5:**  $l_j^{i,k} \leq 0 < u_j^{i,k} \leq t_j^{i,k}$ . Then one can set

$$\beta_j^{i,k} := 0 \quad (53)$$

and only one binary decision variable for the  $j^{\text{th}}$  neuron of the  $k^{\text{th}}$  layer remains. ( $o_j^{i,k}$  lies for sure in the union of the red and blue line segment in Figure 7).

## F.3 MILP for MVNNs with Linear Skip Connection

In this section, we provide a simple extension of the MILP in Theorem 2 for MVNNs with a linear skip connection. First, we define a MVNN with a linear skip connection.

**Definition F.1** (MVNN with Linear Skip Connection). A MVNN with linear skip connection  $\mathcal{M}_i^{\text{lskip},\theta} : \mathcal{X} \rightarrow \mathbb{R}_+$  for agent  $i \in N$  is defined as

$$\begin{aligned} \mathcal{M}_i^{\text{lskip},\theta}(x) = & W^{i,K_i} \varphi_{0,t^{i,K_i}}(\dots \varphi_{0,t^{i,1}}(W^{i,1}x + b^{i,1}) \dots) \\ & + W^{i,0}x, \end{aligned} \quad (54)$$

- $K_i + 1 \in \mathbb{N}$  is the number of layers ( $K_i - 1$  hidden layers),
- $\{\varphi_{0,t^{i,k}}\}_{k=1}^{K_i-1}$  are the MVNN-specific activation functions with cutoff  $t^{i,k} > 0$ , called bounded ReLU (bReLU):

$$\varphi_{0,t^{i,k}}(\cdot) := \min(t^{i,k}, \max(0, \cdot)) \quad (55)$$

- $W^i := (W^{i,k})_{k=0}^{K_i}$  with  $W^{i,k} \geq 0$  and  $b^i := (b^{i,k})_{k=1}^{K_i-1}$  with  $b^{i,k} \leq 0$  are the non-negative weights and non-positive biases of dimensions  $d^{i,k} \times d^{i,k-1}$  (except  $W^{i,0}$  which is of dimension  $d^{i,K_i} \times d^{i,0}$ ) and  $d^{i,k}$ , whose parameters are stored in  $\theta = (W^i, b^i)$ , where  $W^{i,0}$  represents the linear skip connection.

For the MILP of a MVNN with linear skip connection the only thing that changes is the objective, i.e., one needs to replace Equation (8) in Theorem 2 with

$$\max_{a \in \mathcal{F}, z^{i,k}, \alpha^{i,k}, \beta^{i,k}} \left\{ \sum_{i \in N} W^{i,K_i} z^{i,K_i-1} + W^{i,0} z^{i,0} \right\} \quad (56)$$

## G Experiment Details

In this section, we present all details of our experiments from Section 4.

### G.1 SATS domains

In this section, we provide a more detailed overview of the three SATS domains<sup>23</sup>, which we use to experimentally evaluate our new MVNN-based uUB acquisition function in MLCA:

- **Local Synergy Value Model (LSVM)** (Scheffel, Ziegler, and Bichler 2012) has 18 items, 5 *regional* and 1 *national bidder*. Complementarities arise from spatial proximity of items.
- **Single-Region Value Model (SRVM)** (Weiss, Lubin, and Seuken 2017) has 29 items and 7 bidders (categorized as *local*, *high frequency regional*, or *national*) and models large UK 4G spectrum auctions.
- **Multi-Region Value Model (MRVM)** (Weiss, Lubin, and Seuken 2017) has 98 items and 10 bidders (*local*, *regional*, or *national*) and models large Canadian 4G spectrum auctions.

In the efficiency experiments in this paper (i.e., Table 1 and Table 3), we instantiated for each SATS domain the 50 synthetic CA instances with the seeds  $\{10001, \dots, 10050\}$ . We used **SATS version 0.8.0**. All experiments were conducted on a compute cluster running Debian GNU/Linux 10 with Intel Xeon E5-2650 v4 2.20GHz processors with 24 cores and 128GB RAM and Intel E5 v2 2.80GHz processors with 20 cores and 128GB RAM and Python 3.7.10.

### G.2 Hyperparameter Optimization

In this section, we provide details on the exact hyperparameter ranges that we used in our HPO. Table 2 shows all hyperparameter ranges that we used. In the following, we explain selected hyperparameters:

- **DROPOUT PROBABILITY DECAY FACTOR:** After each epoch  $t$  the dropout probability for the next epoch  $t + 1$   $p_{\text{drop}}^{t+1}$  is updated as:  $p_{\text{drop}}^{t+1} = p_{\text{drop}}^t \cdot \kappa$ , where  $\kappa$  denotes this factor.
- **CLIP GRAD NORM:** Parameter for gradient clipping in PYTORCH via `torch.nn.utils.clip_grad_norm(.)`.
- **RANDOM INITIALIZED TS:** Uniform distribution, which is used to initialize the bReLU cutoffs  $t^{i,k}$  i.i.d. uniformly at random, i.e.  $t^{i,k} \sim \text{Unif}(A, B)$  (setting  $A = B$  makes those cutoffs deterministic).
- **TRAINABLE TS:** If set to TRUE, the cutoffs of the bReLU activation function  $\{t^{i,k}\}_{k=1}^{K_i-1}$  are learned (i.e., trained) during the training procedure of the corresponding MVNN.

<sup>23</sup>We do not consider the simplest of all SATS domains, i.e., the **Global Synergy Value Model (GSVM)** (Goeree and Holt 2010), since prior work already achieves 0% efficiency loss without integrating any notion of uncertainty (Weissteiner et al. 2022a), and thus GSVM can be seen as already “solved”.

**Evaluation Metric HPO** We motivate our choice of the two terms in our evaluation metric (15) in the following way:

1. The first term

$$|D^{\text{test}}|^{-1} \sum_{(x,y) \in D^{\text{test}}} \max\{(y - \mathcal{M}_i^{\text{uUB}}(x))q, (\mathcal{M}_i^{\text{uUB}}(x) - y)(1-q)\}$$

of (15) is the standard quantile-loss applied on the test data set. Achieving a low value in this evaluation metric is intuitively desirable since for values  $q > 0.5$  we penalize predictions that are too low more severely than predictions that are too high. It is also theoretically well motivated, since the true<sup>24</sup> posterior  $q$ -credible bound  $\text{uUB}_\alpha(x) := \inf\{y \in \mathbb{R} : \mathbb{P}[\hat{v}_i(x) \leq y | D^{\text{train}}] \geq \alpha\} \forall x \in X$  would minimize this evaluation metric in expectation. As we average this term over 100 different value function and as we use a large test data set for each of them, this is already a good approximation for the expectation.

2. The second term  $\text{MAE}(D^{\text{train}})$  of (15) might appear to be counter-intuitive at first glance, because we are using the training data set. However, for BO it is particularly important to fit well through the noiseless training data points. First, the training data points in BO have already been chosen to lie in a region of potential maximizers. Second, in BO, relative uncertainty (Heiss et al. 2022, Appendix A.2.1.) and particularly Heiss et al. (2022, Desiderata D2) are more important than calibration as discussed in Heiss et al. (2022, Appendix D.2.3). Adding a constant value to  $\mathcal{M}_i^{\text{uUB}}$  would calibrate them but would not change the  $\text{argmax}$  (2) (i.e., would not change the selected queries). However, the 1<sup>st</sup> term of our evaluation metric (15) alone would assign quite low values to  $\mathcal{M}_i^{\text{uUB}}$  of the form  $\mathcal{M}_i^{\text{mean}} + c$ . Fortunately, the second term  $\text{MAE}(D^{\text{train}})$  prevents (15) from assigning low values to  $\mathcal{M}_i^{\text{uUB}}$  of the form  $\mathcal{M}_i^{\text{mean}} + c$ .

### G.3 Details MVNN-Training

Both for the HPO as well as when running an MVNN-based MLCA, we use the following two techniques to achieve numerically more robust results:

1. At the end of the training procedure we use the best weights from all epochs, and not the ones from the last epoch.
2. If at the end of the training procedure the  $R^2$  (coefficient of determination) was below 0.9 on the training set, we retrain once and finally select the model with the best performance across these two attempts.

### G.4 Details MLCA Results

In this section, we provide detailed efficiency loss results when integrating the MVNN-based uUB  $\mathcal{M}_i^{\text{uUB}}$  in MLCA. Specifically, we present in Table 3 efficiency loss results for all four HPO winner configurations (with respect to the evaluation metric based on the four different quantile parameters

<sup>24</sup>By “true posterior” we denote the posterior coming from the “true prior” that we sample our value functions  $\hat{v}_i$  from.

CATEGORY	HYPERPARAMETER	RANGE	LOG-UNIFORM SAMPLING
DATA	NUMBER OF TRAINING DATA POINTS: $ D^{\text{TRAIN}} $	LSVM: 50 SRVM: 100 MRVM: 100	
	NUMBER OF TEST DATA POINTS: $ D^{\text{TEST}} $	LSVM: $2^{10}$ SRVM: $2^{13}$ MRVM: $2^{13}$	
	NUMBER OF SATS INSTANCES	100	
GENERIC MVNN	ARCHITECTURE: (#NEURONS PER HIDDEN LAYER, #HIDDEN LAYERS)	LSVM: {(96, 1), (32, 2), (16, 3)} SRVM: {(32, 2), (16, 3)} MRVM: {(96, 1), (64, 1), (20, 2)}	
	LINEAR SKIP CONNECTION (SEE DEFINITION F.1)	{TRUE, FALSE}	
	BATCH SIZE	$\{ D^{\text{TRAIN}} /4,  D^{\text{TRAIN}} /2,  D^{\text{TRAIN}} \}$	
	EPOCHS	$\{4000 \frac{\text{BATCH SIZE}}{ D^{\text{TRAIN}} }, 4500 \frac{\text{BATCH SIZE}}{ D^{\text{TRAIN}} }, 5000 \frac{\text{BATCH SIZE}}{ D^{\text{TRAIN}} }, \dots, 8000 \frac{\text{BATCH SIZE}}{ D^{\text{TRAIN}} }\}$	
	DROPOUT PROBABILITY	[0, 0.8]	
	DROPOUT PROBABILITY DECAY FACTOR	[0.75, 1.0]	
	OPTIMIZER	ADAM	
GENERIC LOSS	LEARNING RATE	GSVM: [0.0002, 0.002] LSVM: [0.001, 0.01] SRVM: [0.0008, 0.006] MRVM: [0.0007, 0.004]	YES
	L2-REGULARIZATION: $\lambda$ (SEE EQUATION (6))	[1E-10, 1E-3]	YES
	SMOOTH L1-LOSS $\beta$ (SEE DEFINITION D.1)	{1/32, 1/64, 1/128}	
	CLIP GRAD NORM	[1E-6, 1]	YES
	NUMBER OF ARTIFICIAL INPUT DATA POINTS: $ D^{\text{ART}} $ (SEE SECTION 3.1)	{64,80,96, ..., 512}	
NEW NOMU LOSS	$\pi_{\text{SOR}}$ (SEE EQUATION (6))	1	
	$\pi_{\text{EXP}}$ (SEE EQUATION (6))	[1E-6, 5E-1]	YES
	$\underline{\pi}$ (SEE EQUATION (6))	[64, 256]	YES
	$\bar{\pi}$ (SEE EQUATION (6))	0.25	
	$c_{\text{EXP}}$ (SEE EQUATION (6))	[64, 256]	YES
MVNN INITIALIZATION	RANDOM INITIALIZED TS	UNIF(0,1)	
	TRAINABLE TS	{TRUE, FALSE}	
	INITIAL EXPECTATION: $\mathbb{E}^{\text{INIT}}$ (SEE APPENDIX E.2)	[1, 2]	
	INITIAL VARIANCE: $\mathbb{V}^{\text{INIT}}$ (SEE APPENDIX E.2)	[0.02, 0.16]	YES
	INITIAL BIAS: $b^{\text{INIT}}$ (SEE APPENDIX E.2)	0.05	
	INITIAL "B" CONSTANT: $B^{\text{INIT}}$ (SEE APPENDIX E.2)	0.05	
	INITIAL "LITTLE" CONSTANT: $\epsilon$ (SEE APPENDIX E.2)	0.1	

Table 2: Hyperparameter ranges used in our HPO for random search. If not explicitly stated otherwise, the ranges apply to all considered SATS domains.

DOMAIN	QUANTILE PARAMETER Q	$Q^{\text{INIT}}$	$Q^{\text{ROUND}}$	$Q^{\text{MAX}}$	EFFICIENCY LOSS IN % $\downarrow$	REVENUE IN % $\uparrow$	RUNTIME IN HOURS
LSVM	0.60	40	4	100	0.69 $\pm$ 0.41	74.73 $\pm$ 3.68	4.90
	0.75	40	4	100	0.69 $\pm$ 0.44	75.07 $\pm$ 3.71	5.53
	0.90	40	4	100	0.39 $\pm$ 0.30	73.53 $\pm$ 3.72	15.64
	0.95	40	4	100	0.40 $\pm$ 0.35	73.88 $\pm$ 3.93	15.58
SRVM	0.60	40	4	100	0.16 $\pm$ 0.04	54.34 $\pm$ 1.48	24.67
	0.75	40	4	100	0.06 $\pm$ 0.02	54.22 $\pm$ 1.46	18.80
	0.90	40	4	100	0.54 $\pm$ 0.08	53.89 $\pm$ 1.44	33.90
	0.95	40	4	100	0.62 $\pm$ 0.11	54.25 $\pm$ 1.54	33.26
MRVM	0.60	40	4	100	7.88 $\pm$ 0.43	41.81 $\pm$ 1.06	61.48
	0.75	40	4	100	8.44 $\pm$ 0.43	41.89 $\pm$ 0.93	34.91
	0.90	40	4	100	7.77 $\pm$ 0.34	42.04 $\pm$ 0.89	28.15
	0.95	40	4	100	7.98 $\pm$ 0.34	42.28 $\pm$ 1.00	27.92

Table 3: Efficiency loss, relative revenue and runtime of MLCA with our MVNN-based uUB  $\mathcal{M}_i^{\text{uUB}}$  as acquisition function. Shown are averages including a 95%-normal-CI on a test set of 50 instances in all three considered SATS domains. The best MVNN-based uUBs per domain based on the lowest efficiency loss are marked in grey.

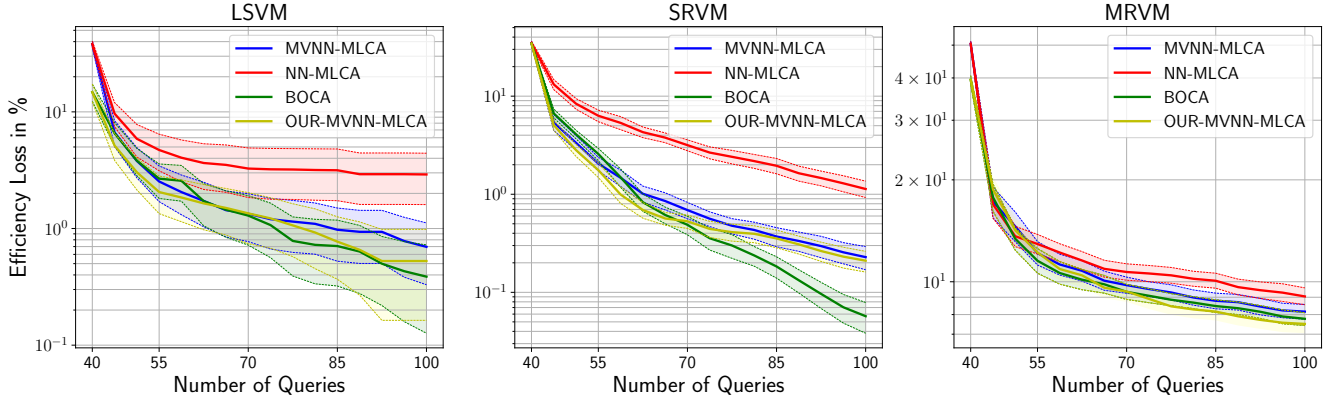


Figure 8: Efficiency loss paths (i.e., regret plots) of MLCA with OUR-MVNNs (yellow) compared to NOMU-MVNNs and to the results from Weissteiner et al. (2022a) of MVNNs and plain NNs. Shown are averages with 95% CIs over 50 instances.

$q \in \{0.6, 0.75, 0.9, 0.95\}$ ). Furthermore, we present the *relative revenue*  $\sum_{i \in N} p(R)_i / V(a^*)$  of an allocation  $a_R^* \in \mathcal{F}$  and payments  $p(R) \in \mathbb{R}_+^n$  determined by MLCA using our MVNN-based uUB  $\mathcal{M}_i^{\text{uUB}}$  when eliciting reports  $R$  as well as the average runtime in hours for a single instance (i.e., how long it would take to run a single auction). Note that since we stop MLCA when we have already found an allocation with 0% efficiency loss, the relative revenue numbers (in LSVM and SRVM) are pessimistic and typically increase if we let MLCA run until  $Q^{\max}$  is reached. For the runtime results the opposite holds.

**Revenue** Comparing the revenue of our BOCA (see Table 3) to the revenue of MVNN-MLCA and NN-MLCA in Weissteiner et al. (2022a, Table 6), we see that overall the mean relative revenue is as good or better than SOTA. For LSVM (and SRVM) this comparison could be flawed because we stop computing further queries when reaching 0% efficiency loss as described above.

However, for MRVM, we always compute all 100 queries as can be seen in Weissteiner et al. (2022a, Table 6). Thus MRVM allows for a fair comparison of the relative revenue. For MRVM BOCA’s relative revenue is on average  $\sim 7\%$ -points higher than the one of MVNN-MLCA. With a confidence of more than 95% the revenue of BOCA is by more than 4%-points (corresponding to  $\sim 200$  million USD in this domain<sup>25</sup> (Ausubel and Baranov 2017)) better than the one of MVNN-MLCA. The comparison of BOCA to NN-MLCA is also in favour of BOCA, but much closer (and BOCA outperform NN-MLCA in terms of social welfare with a  $p_{\text{VAL}} = 2e-5$ , see Table 1).

The strength of BOCA with respect to revenue is quite intuitive since each query that explores regions of high uncertainty in the bundle space is beneficial for all economies, while “exploiting” an allocation which leads to high effi-

ciency in one certain economy is mainly beneficial for this certain economy (see Appendix A for the definition of main and marginal economies). As discussed in Weissteiner et al. (2022a, Appendix E.3), MLCA queries the main economy more often than any other economy and revenue is high if the social welfare in the marginal economies is high relative to the social welfare in the main economy. Thus, exploration favours high revenue in settings (such as ours) where the main economy is queried more often than the marginal economies.

### G.5 Disentangling BOCA’s Performance Increase

In this section, we present further efficiency loss paths plots when using only the mean MVNN  $\mathcal{M}_i^{\text{mean}}$  of  $\mathcal{M}_i^{\text{NOMU}}$  in MLCA. We call this method OUR-MVNN-MLCA. Note that OUR-MVNN-MLCA does not integrate any notion of uncertainty and is thus the same method as MVNN-MLCA from Weissteiner et al. (2022a), but now with our new proposed parameter initialization method (see Section 3.2) and optimized with our HPO.

In Figure 8, we present the efficiency loss path plots for OUR-MVNN-MLCA (yellow) compared to the results presented in Figure 4 in the main paper. As expected, we see that BOCA, i.e., integrating a notion of uncertainty, is as good or better than OUR-MVNN-MLCA, i.e., only using the mean model. This effect is statistically significant in SRVM, while in LSVM and MRVM both lead to results that are statistically on par. The degree to which exploration via a notion of uncertainty is beneficial depends on intrinsic characteristics of the domain (e.g., the dimensionality). Specifically, in MRVM where the query budget of  $Q^{\max} = 100$  is extremely small compared to the dimensionality of the domain (i.e., MRVM has  $m = 98$  items and  $n = 10$  bidders thus the dimensionality is  $980 = 98 \cdot 10$ ), we see that exploitation might be beneficial compared to adding exploration (De Ath et al. 2021) and the power of adding exploration may reveal itself only when increasing the query budget. However, in LSVM and SRVM ( $m = 18$  and  $m = 29$ ), we see that adding exploration with a uUB  $\mathcal{M}_i^{\text{uUB}}$  decreases the efficiency loss. Finally, these results also suggest that our

<sup>25</sup>The revenue of the 2014 Canadian 4G auction was  $\sim 5$  billion USD (Ausubel and Baranov 2017) and MRVM simulates exactly this specific auction. Thus, 4%-points of 5 billion USD corresponds to  $\sim 200$  million USD. If one accumulates the revenue of all spectrum auctions one would obtain significantly larger values.

proposed new parameter initialization method for MVNNs discussed in Section 3.2 tends to be better than a simple generic one, since OUR-MVNN-MLCA is on average better than MVNN in every domain.